NASA TN D-317

TECHNICAL NOTE
D-317

WIND-TUNNEL TESTS OF A CIRCULAR WING WITH AN ANNULAR NOZZLE IN PROXIMITY TO THE GROUND

By Richard K. Greif, Mark W. Kelly, and
William H. Tolhurst, Jr.

Ames Research Center
Moffett Field, Calif.

NATIONAL AERONAUTICS AND SPACE ADMINISTRATION

WASHINGTON

May 1960

NATIONAL AERONAUTICS AND SPACE ADMINISTRATION

TECHNICAL NOTE D-317

WIND-TUNNEL TESTS OF A CIRCULAR WING WITH AN ANNULAR NOZZLE IN PROXIMITY TO THE GROUND

By Richard K. Greif, Mark W. Kelly, and
William H. Tolhurst, Jr.

SUMMARY

Exploratory wind-tunnel tests have been conducted to determine the effect of forward speed on the vertical thrust of an annular nozzle exhausting toward the ground. The model consisted of a 19-inch-diameter annular nozzle housed in the lower surface of a 22-inch-diameter, 6-percent-thick, circular wing. Measurements of lift, drag, and pitching moment were obtained at various angles of attack for altitudes from 1 to 50 inches, free-stream dynamic pressures from 0 to 30 pounds per square foot, and nozzle pressure ratios from 1.0 to 2.0. Measurements were also made to determine pressure profiles on the nozzle base plate and on the ground.

The results from tests at zero forward speed show that the model experienced thrust augmentation near the ground. Thrust values varied from one-half the jet momentum at high altitudes to three times the jet momentum at an altitude of 1/20 the nozzle diameter. The effect of forward speed on vertical thrust depended on the distance of the nozzle from the ground. Near the ground, forward speed could increase or decrease the thrust, depending on the conditions of altitude, forward speed, and jet momentum considered. Far from the ground, the effect of forward speed was favorable and always increased thrust. With the moment center located at the center of the wing, this configuration was statically unstable longitudinally for all conditions of altitude and forward speed.

INTRODUCTION

As an annular nozzle approaches the ground, its hollow cylindrical jet forms an aerodynamic enclosure between the nozzle base plate and the ground. The nature of the resulting flow, as shown in reference 1, is such that a pressure increase occurs within the enclosure, causing a vertical force on the nozzle base plate. Since this force adds to the reactive force due to the jet, the annular nozzle is said to experience a thrust augmentation in proximity to the ground. A simplified theoretical explanation of this phenomenon is presented in reference 2. Additional information on the subject may be found in references 3 through 6.

Since the magnitude of thrust augmentation increases with decreasing altitude, the annular nozzle is capable of providing vertical thrust which greatly exceeds the momentum in its jet. Efforts are therefore being made to determine the feasibility of incorporating the annular nozzle concept into some form of airborne vehicle, either as the main lifting force for a very low flying vehicle, or as an aid in the landing and take-off of conventional aircraft. In any case, with the exception of a pure VTOL application, it is necessary to determine to what degree thrust augmentation is maintained when the annular nozzle is operated at forward speeds.

In view of the foregoing, an exploratory wind-tunnel test was conducted on an annular nozzle housed in the lower surface of a thin circular plan-form wing. The primary purpose of the investigation was to determine the effect of forward speed on the vertical thrust of the model in proximity to the ground. Additional measurements were included to determine the longitudinal aerodynamic characteristics of the configuration. The tests were of a preliminary type and their quantitative interpretation requires consideration of the remarks contained in the section entitled, "Corrections."

NOTATION

$\bar{c}$	mean aerodynamic chord, 1.66 ft
C_D	drag coefficient, $\frac{\text{drag}}{q_\infty S}$
C_L	lift coefficient, $\frac{\text{lift}}{q_\infty S}$
ΔC_L	increment of lift coefficient due to blowing from annular nozzle
C_m	pitching-moment coefficient, $\frac{M}{q_\infty S\bar{c}}$
C_μ	jet momentum coefficient, $\frac{m_j V_j}{q_\infty S}$
D_o	outside diameter of annular nozzle slot, 18.9 in.
h	nozzle altitude (distance from nozzle base plate to ground), in.
m_j	mass rate of flow in the jet, slugs/sec
M	pitching moment, ft-lb
p	static pressure, psia
p_t	total pressure, psia
q	dynamic pressure, psf
S	wing area, 2.64 sq ft

r	radius, in.
r_o	outside radius of annular nozzle slot, 9.45 in.
t	thickness of annular slot, 0.11 in.
T_v	vertical thrust measured in direction perpendicular to ground, lb
T_h	horizontal thrust measured in direction parallel to ground, lb
T_j	calculated jet momentum thrust, $m_j v_j$, lb
v	velocity, fps
α	angle of attack of wing-chord plane, deg

Subscripts

j	annular jet
∞	free stream
l	local

MODEL AND APPARATUS

Model

The model consisted of a 22-inch-diameter, circular plan-form wing with an annular nozzle in its lower surface. Details and major dimensions of the model are shown in figure 1(a), along with a table of ordinates for a radial section of the model. Figure 1(b) shows the location of the pressure orifices used to obtain pressure data on the ground plane and the nozzle base plate.

The circular wing was symmetrical about its principal axes and had a thickness ratio of 0.06 based on its major diameter. The aspect ratio was $4/\pi$ and the mean aerodynamic chord was 1.66 feet. The moment center, about which pitching moments were computed, was located at the center of the model.

The annular nozzle was a convergent type designed to exhaust normal to the chord plane of the wing. The nozzle slot was 0.11 inch wide and had an outside diameter of 18.9 inches.

The geometry of the wing and the nozzle remained unchanged throughout the test.

Wind-tunnel installation.- The circular wing and ground plane were arranged in the Ames 7- by 10-foot wind tunnel as shown in the photograph of figure 2(a). The photograph of figure 2(b) shows the annular nozzle in the wing lower surface.

The model was supported by its air supply line, which was fastened to the center of the balance frame turntable. Wing angle of attack was varied by rotating the turntable. Wing altitude was varied by fastening the plywood ground plane at various lateral locations in the tunnel. The ground plane, extending 4 feet fore and aft of the model center line and from top to bottom of the tunnel, was always positioned parallel to the tunnel's vertical plane of symmetry.

A rotating seal beneath the turntable was used to join the external air supply line to the model support line. Although flexible couplings were used in the external line in order to isolate it from the balance system, extraneous forces were introduced when the line was pressurized. These forces were calibrated against line pressure and applied as a correction in the results.

A fairing was installed to eliminate drag forces on the vertical section of the model support line. However, the short horizontal section after the elbow was not protected by a fairing and the data presented herein include the aerodynamic force on this portion of the air supply line.

Instrumentation

A conventional mechanical balance was used to obtain measurements of the aerodynamic forces on the model.

Measurement of jet momentum, $m_j v_j$.- The mass flow rate, m_j, of air through the nozzle was determined by means of a sharp-edged orifice located in the external air supply line. Nozzle exit total pressure was indicated by a single total pressure probe in the model support line which had been calibrated against nozzle exit total pressures measured by circumferential surveys of the nozzle annulus. The jet velocity v_j, then, was calculated assuming an isentropic expansion from p_{t_j} to p_∞. When the probable errors in m_j and v_j are taken into consideration, it is estimated that the computed values of jet momentum are accurate to within approximately ±7 percent.

PROCEDURE

Range of Variables

Force data along with nozzle air-flow and pressure measurements were obtained over a range of tunnel free-stream dynamic pressures from 0 to

30 pounds per square foot. The model was tested at nine altitudes, ranging from 1 to 50 inches (h/D_o from 0.05 to 2.65). Nozzle exit pressure ratio, p_{t_j}/p_∞, was varied from 1 (no jet flow) to 2. Combinations of tunnel free-stream dynamic pressure and nozzle exit pressure produced a range of jet momentum coefficients from 0 to ∞. The range of wing angles of attack was -24^o to $+24^o$, except in cases when wing stall or ground plane contact was encountered first.

Method of Testing

Zero forward speed case.- In the tests at zero forward speed, data over a range of p_{t_j}/p_∞ from 1.17 to 1.68 were obtained at 0^o angle of attack for each of the nine altitudes. The tests to determine the effect of angle of attack on T_v/T_j were conducted at a constant p_{t_j}/p_∞ of 1.34.

Forward speed case.- Early in the tests it was determined that the aerodynamic characteristics of the model at forward speeds were functions only of altitude, angle of attack, and the momentum coefficient of the jet. Since C_μ is a single-valued function of the ratio of p_{t_j} to q_∞, it was unnecessary to determine the individual effects of these variables, and the amount of testing was greatly reduced. The data at each altitude were obtained simply by holding constant values of C_μ over ranges of angles of attack.

CORRECTIONS

In view of the preliminary nature of the tests, no corrections for wind-tunnel wall effects have been applied to the results. The interpretation of the results should also take into consideration the following factors:

1. The presence of a boundary layer on the ground plane during forward speed tests creates some question as to the validity of the wind-tunnel simulation. For the conditions of this test the thickness of the boundary layer was estimated from turbulent boundary-layer theory to be approximately 3/4 inch at a ground plane station below the leading edge of the model. In addition to its effect on the interaction between the jet and the free stream, the boundary layer probably caused some upward inclination of the free stream. Based on the displacement thickness of the boundary layer (approximately 1/4 in.), the inclination of the free stream was estimated to be about 0.4^o.

2. The altitudes listed with the results were measured before each run while no forces were acting on the model. During the tests, however,

forces on the model caused some deflection of the model strut and thereby a change in altitude. Measurements of the strut deflection have resulted in the following corrections for h/D_o:

a. At zero forward speed,

$$\Delta(h/D_o) \approx T_v \times 10^{-4}$$

where

$$T_v = (T_v/T_j)T_j$$

$$T_j \approx 150[(p_{t_j}/p_\infty) - 1]$$

b. At forward speeds,

$$\Delta(h/D_o) \approx C_L q_\infty S \times 10^{-4}$$

where (unless otherwise indicated):

$$q_\infty = 10 \quad \text{for} \quad C_\mu > 3$$

$$q_\infty = 20 \quad \text{for} \quad C_\mu < 3$$

Except at altitudes less than $h/D_o = 0.1$, the above corrections are negligible.

3. The direct aerodynamic forces on the exposed section of the supply air strut and the interference effect of the strut on the wing are included in the results. The direct aerodynamic forces are estimated to cause C_D to be approximately 0.09 too positive and C_m to be approximately 0.02 too positive. No attempt has been made to estimate the strut interference effect on C_D or C_m.

4. An additional consideration regarding C_m is the fact that the balance system used in the test was not designed to measure such small pitching moments. As a result, C_m is only accurate to about ±0.03 at the lowest speed tested.

RESULTS

In order to provide a meaningful evaluation of the contribution of the annular nozzle to the lift of the circular wing, measured vertical thrust is compared to the momentum in the jet by presenting the results in the form of a thrust-momentum ratio. At zero forward speed, this thrust-momentum ratio is represented by T_v/T_j. At finite forward speeds, the ratio $\Delta C_L/C_\mu$ is used, where ΔC_L is the measured increase in lift coefficient due to the annular jet, and C_μ is the jet momentum expressed

in coefficient form to be consistent with C_L. Then $\Delta C_L/C_\mu$ is the forward speed equivalent of T_V/T_j, and the two can be compared directly. The terms thrust augmentation and thrust reduction appearing in the discussion are used to refer to values of T_V/T_j (or $\Delta C_L/C_\mu$) greater and less than unity, respectively.

Operation of the Model at Zero Forward Speed

The variation of vertical thrust-momentum ratio, T_V/T_j, with altitude in terms of h/D_o, for the nozzle operating at zero forward speed, is shown in figure 3. These data were obtained at 0^o angle of attack and at values of nozzle pressure ratio ranging from 1.17 to 1.68. Since the variations in T_V/T_j due to changes in p_{t_j}/p_∞ are within the estimated error in the data, it appears that T_V/T_j is independent of nozzle pressure ratio for nozzles of this ratio of nozzle area to base area. The resulting single curve shows that, at altitudes greater than about one diameter of the nozzle annulus (h/D_o greater than 1), the thrust of the annular nozzle was only about 50 percent of the momentum in its jet. However, operation of the annular nozzle at altitudes nearer to the ground (h/D_o less than 1) reveals the presence of a favorable ground effect on thrust. The strength of this ground effect is seen to be sufficient to produce thrust augmentation at altitudes less than half the annulus diameter (h/D_o less than 0.5). The amount of thrust augmentation was only moderate ($T_V/T_j = 1.3$), however, until h/D_o became less than 0.1. At this point, T_V/T_j increased rapidly with decreasing h/D_o. At the lowest test altitude, the vertical thrust-momentum ratio reached a value of approximately 3.

Also shown in figure 3 are curves of T_V/T_j vs. h/D_o representing the thin-jet theory of reference 2 and the experimental results from figure 6 of reference 1. (The abscissa, h/D_b, used in fig. 6, ref. 1, has been converted to h/D_o.) While the three curves in figure 3 show qualitative agreement, significant differences are apparent. The theoretical curve, for example, was derived for an infinitely thin annular jet; yet, the annular nozzle of reference 1, which produced a relatively thick jet ($t/D_o = 0.084$), comes closer to achieving the thrust values predicted by the theory than does the thin nozzle ($t/D_o = 0.0058$) of this report. And, although both nozzles exhibit thrust reduction out of the ground effect (a phenomenon unaccounted for in the theory of reference 2, although it is discussed therein), the nature of their transition to thrust augmentation differs. Once thrust augmentation has been achieved, the thrust of the thick nozzle varies in an always increasing manner, while the thin nozzle experiences a thrust peak at $h/D_o = 0.4$. (Similar thrust peaks were observed in preliminary tests with other thin nozzles, but the cause of their occurrence is unexplained.) In view of the foregoing dissimilarities at zero forward speed, it should be noted that there is a possibility that the forward speed results which follow would not apply to annular nozzles producing thicker jets.

The effect of angle of attack on T_V/T_j for several altitudes is presented in figure 4(a). Since the results of figure 3 showed the effect of nozzle pressure ratio to be negligible, the data in figure 4(a) were obtained at a constant p_{t_j}/p_∞ of 1.34. Angle of attack is seen to cause a loss in T_V/T_j, the loss becoming larger as the nozzle approaches lower altitudes. (The slight asymmetry in these curves is probably due to non-uniformity in the nozzle annulus and/or errors in alining the ground plane to be parallel with the model.) For h/D_o above 1, the variation of T_V/T_j with α closely approximates (as expected) a cosine curve.

Operation of the nozzle at various angles of attack also produced changes in horizontal thrust and pitching moment. This is shown in figure 4(b); of particular interest in this figure is the fact that stability in pitch varies from neutral out of the ground effect to unstable in the ground effect.

Operation of the Model at Forward Speed

In establishing parameters for the forward speed tests of the model, it was reasoned that the thrust-momentum ratio, $\Delta C_L/C_\mu$, could be completely determined by altitude (h/D_o), angle of attack (α), and some parameter containing forward speed and jet velocity. A logical choice for the latter appeared to be, from dimensional considerations, the ratio of v_j/v_∞. Also, since the square of v_j/v_∞ is proportional to C_μ, it followed that h/D_o, α, and C_μ would be sufficient to determine $\Delta C_L/C_\mu$. The foregoing reasoning is verified by the results in figure 5 showing the variation of $\Delta C_L/C_\mu$ with C_μ for various altitudes. Similar correlations with C_μ were obtained for C_D and C_m. The data were obtained over a range of nozzle pressure ratios (determining v_j) from 1.17 to 2.02, a range of q_∞ (determining v_∞) from 5 to 30 psf, and at a constant angle of attack of 0^o. Since similar results were obtained at positive and negative angles, it can be concluded that $\Delta C_L/C_\mu$ is, within the limits of this investigation, determined solely by h/D_o, α, and C_μ.

The manner is which the thrust momentum ratio is affected by increasing forward speed is also indicated in figure 5, since, for constant p_{t_j}/p_∞, v_∞ varies with the inverse of C_μ. With the model operating out of the ground effect ($h/D_o = 2.65$), it is seen that $\Delta C_L/C_\mu$ increases with decreasing C_μ (increasing v_∞). However, with the model operating in the ground effect ($h/D_o = 0.11$ and 0.42) it is seen that $\Delta C_L/C_\mu$ is not affected by forward speed so long as C_μ is larger than about 3; for lower C_μ a reduction in $\Delta C_L/C_\mu$ results.

The forward speed performance of the model at 0^o angle of attack is also shown in figure 6. This figure presents the variation of thrust-momentum ratio, $\Delta C_L/C_\mu$, with altitude for various values of C_μ ranging from 0.45 to infinity. (The curve $C_\mu = \infty$ was transposed from fig. 3, since for $q_\infty = 0$, $C_\mu = \infty$ and $T/T_j = \Delta C_L/C_\mu$.) As before, the effect on

$\Delta C_L/C_\mu$ due to increasing forward speed can be obtained in figure 6 from an examination of the effect of decreasing C_μ. The effects of forward speed are generally the same as discussed in the previous paragraph. When the model is operated out of the ground effect, increasing forward speed has a definitely favorable effect on $\Delta C_L/C_\mu$ which eventually results in complete recovery of the thrust loss suffered at these altitudes in the zero forward speed condition. When the model is operated near the ground, effects of forward speed are not as clearly defined and depend, to a large degree, on h/D_o. As C_μ is decreased it appears that $\Delta C_L/C_\mu$ at first decreases to a minimum value, and then increases with further decreases in C_μ. Thus the over-all effect of forward speed on the thrust-momentum ratio of this configuration was favorable out of the ground effect, and either favorable or unfavorable in the ground effect, depending on the values of h/D_o and C_μ being considered. It should be noted that there is some question regarding the relative positions of the points for $h/D_o = 0.05$, since considerable forces were acting on the model and noticeable bending of the model strut occurred. (See item 2 in section entitled "Corrections.") Thus, for increasing C_μ's the model was probably operating at altitudes increasingly greater than an h/D_o of 0.05. The possibility exists, then, that the position of the points might have been reversed if the strut had not deflected.

Longitudinal Aerodynamic Characteristics of the Model

The lift, drag, and pitching-moment characteristics of the model are shown in figures 7(a) through 7(i). These figures are plotted in the conventional form showing α, C_D, and C_m versus C_L. The data in each figure were obtained at a constant altitude. The altitudes presented vary from $h/D_o = 0.05$ (fig. 7(a)) to $h/D_o = 2.65$ (fig. 7(i)). The data for the individual curves in each figure were obtained at a constant jet momentum coefficient; C_μ ranged from 0 (blowing off) to approximately 5.5. It is seen in figure 7 that the circular wing and annular nozzle combination is unstable in pitch throughout the entire range of α, h/D_o, and C_μ covered in the tests. In addition to the ground effect phenomenon discussed in the previous section, h/D_o and C_μ had pronounced effects on the behavior of the lift curve (C_L vs. α). The slope of the lift curve is seen to increase with decreasing h/D_o and increasing C_μ. The angle of attack for maximum lift, on the other hand, decreases with decreasing h/D_o and increasing C_μ. The drag coefficient values in figure 7 are believed to be approximately 0.09 high since no correction was made to account for the short horizontal section of the strut which was exposed to the free stream.

Pressure Ratio Distributions

Pressure ratio profiles developed in the streamwise plane of symmetry both on the nozzle base plate and on the ground plane are shown in

figures 8, 9, and 10 for the model operating at three representative altitudes: $h/D_o = 0.11$, $h/D_o = 0.42$, and $h/D_o = 2.65$, respectively. Part (a) of each figure shows the effect of C_μ on the pressure profiles for operation of the model at 0^o angle of attack. The (b) and (c) parts show the effect of α on the pressure profiles for operation of the model at constant C_μ of 1.9 and ∞, respectively. In interpreting the figures, an abscissa is shown in each to represent the nozzle base plate with a wider abscissa below it to represent the ground plane. The units of each are shown in terms of a dimensionless radial distance, r/r_o, from the model center line. Pressures have been made dimensionless in figures 8, 9, and 10 by dividing each local pressure, $p_l - p_\infty$, by the nozzle exit pressure, $p_{t_j} - p_\infty$. Positive ratios of $(p_l - p_\infty)/(p_{t_j} - p_\infty)$ are shown in directions away from each surface; that is, positive $(p_l - p_\infty)/(p_{t_j} - p_\infty)$ on the nozzle base plate is measured down from its corresponding abscissa, while positive $(p_l - p_\infty)/(p_{t_j} - p_\infty)$ on the ground plane is measured up.

The pressure-distribution data are presented essentially without discussion. They have been included in the report for the primary purpose of providing gross indications of the effects of C_μ and α on the flow patterns of the annular jet. Additional use of these data to explain aerodynamic forces at forward speeds (finite C_μ) is seriously restricted because of the absence of pressure data on the model upper surface. At zero forward speed (infinite C_μ), however, the pressure forces on the model upper surface are negligible, so that the pressure data presented here are useful in supporting previous results. For example, the thrust augmentations shown at h/D_o of 0.11 and 0.42 in figure 3 are clearly indicated to be the results of positive pressure forces on the nozzle base plate. In addition, the pressure data at various α can be used to explain the stability results shown in figure 4(b). The thrust reduction at altitudes out of the ground effect is shown in figure 10(a) (top) to be the result of negative pressure forces on the nozzle base plate. Also, a jet instability occurred at this condition (as indicated by the band of pressure data) causing asymmetric and varying loads on the nozzle base plate.

SUMMARY OF RESULTS

Wind-tunnel tests of a 22-inch-diameter, thin, circular wing with an annular nozzle exhausting from its lower surface were conducted in the Ames 7- by 10-foot wind tunnel. The annular nozzle had an outside diameter of 18.9 inches, a slot thickness of 0.11 inch, and was designed to exhaust normal to the wing chord plane. The principal results of these tests are summarized in the following.

1. The results from zero forward speed tests are in general agreement with the results of reference 1 showing that annular nozzles experience a thrust augmentation due to a favorable effect of ground proximity. Thrust

values ranged from one-half the jet momentum at altitudes greater than one nozzle diameter to about three times the jet momentum at an altitude of 1/20 the nozzle diameter. The exact manner in which thrust varied with altitude differs from that reported in reference 1, probably because of a difference in the ratio of nozzle area to enclosed base area. (In the tests of ref. 1 the jet was much thicker.)

2. The results from tests at forward speed show that for operation of the model near the ground, the effect of forward speed could be favorable or unfavorable, depending on the particular values of altitude, forward speed, and jet momentum considered. For operation far from the ground, increasing forward speed always increased thrust.

3. With moments taken about its center, the model was statically unstable longitudinally for the altitudes and forward speeds tested in this investigation.

Ames Research Center
National Aeronautics and Space Administration
Moffett Field, Calif., Jan. 14, 1959

REFERENCES

1. Von Glahn, Uwe H.: Exploratory Study of Ground Proximity Effects on Thrust of Annular and Circular Nozzles. NACA TN 3982, 1957.

2. Chaplin, Harvey R.: Theory of the Annular Nozzle in Proximity to the Ground. DTMB Aero. Lab., Aero. Rep. 923, 1957.

3. Chaplin, Harvey, R., and Stephenson, Bertrand: Preliminary Study of the Hovering Performance of Annular Jet Vehicles in Proximity to the Ground. DTMB Aero. Lab., Aero. Rep. 947, 1958.

4. Boehler, Gabriel D., and Spindler, Robert J.: Aerodynamic Theory of the Annular Jet (Part I). Aerophysics Co. Rep. AR 581-R, 1958.

5. Rethorst, Scott, and Royce, W. W.: Lifting Systems for VTOL Vehicles. IAS Paper No. 59-123, 1959.

6. Matthews, G. B., and Wosser, J. L.: Ground Proximity: A Critical Review. IAS Paper No. 59-121, 1959.

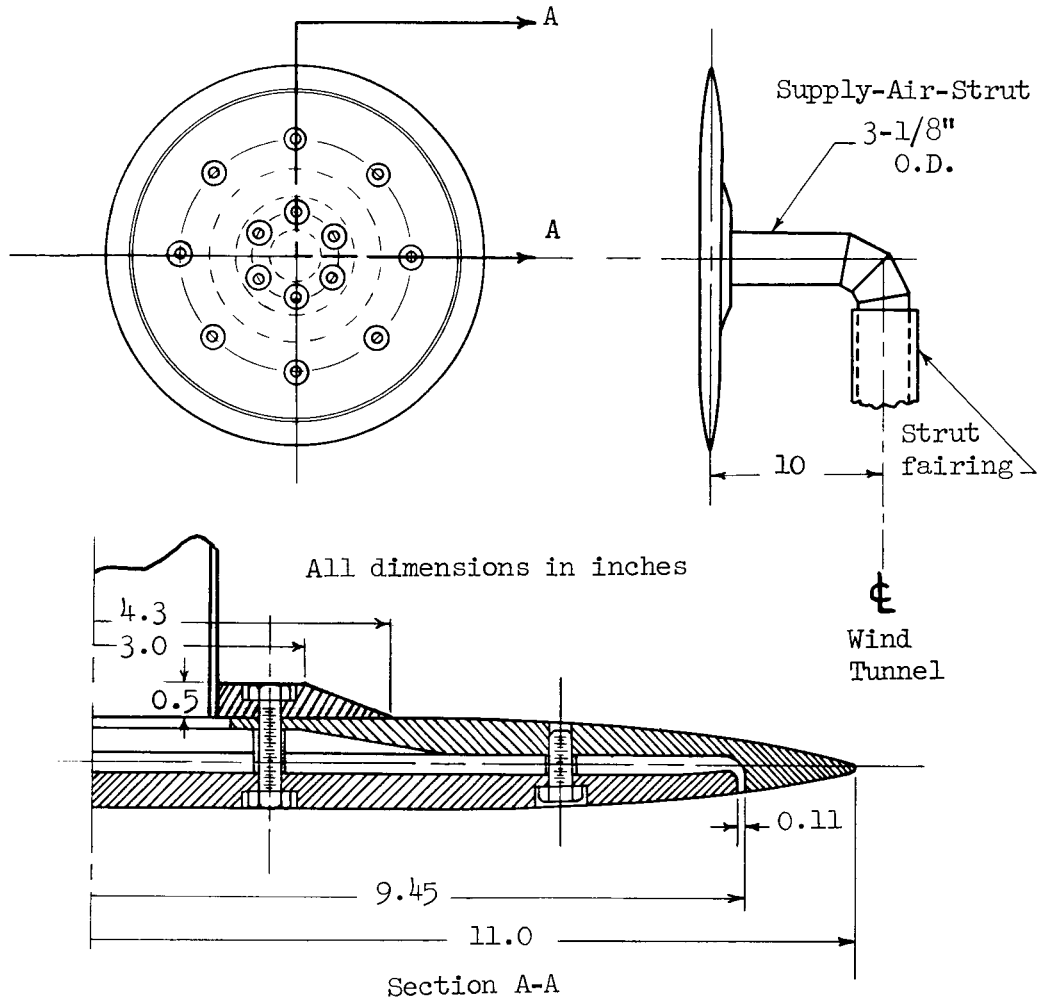

Coordinates for All Radial Sections		
Radial Dist. From Center r inches	Dist. to Upper or Lower Surface y inches	
0	0.66	Flat Surface
5.00	0.66	
6.00	0.644	Surface of Constant Radius of Curvature = 30.4"
7.00	0.594	
8.00	0.512	
9.00	0.396	
10.00	0.246	
Edge Radius = 1/16 inch		

(a) Major dimensions.

Figure 1.- Details of the circular wing with annular nozzle model.

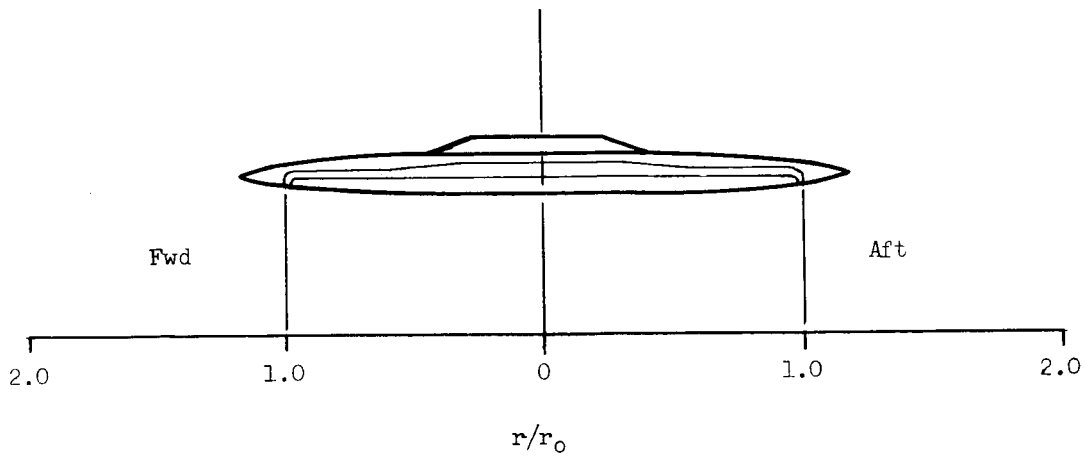

Longitudinal location of orifices		
On nozzle base plate r/r_o		On ground plane r/r_o
		1.91
		1.69
		1.48
	Aft	1.27
0.93		1.06
0.79		0.85
0.64		0.64
0.42		0.42
0.21		0.21
0		0
0.21		0.21
0.42		0.42
0.64		0.64
0.79		0.85
0.93		1.06
	Fwd	1.27
		1.48
		1.69
		1.91

Note: All orifices were located in the streamwise plane of symmetry.

(b) Location of pressure orifices in nozzle base plate and ground plane.

Figure 1.- Concluded.

A-24889

(a) General arrangement of circular wing and ground plane.

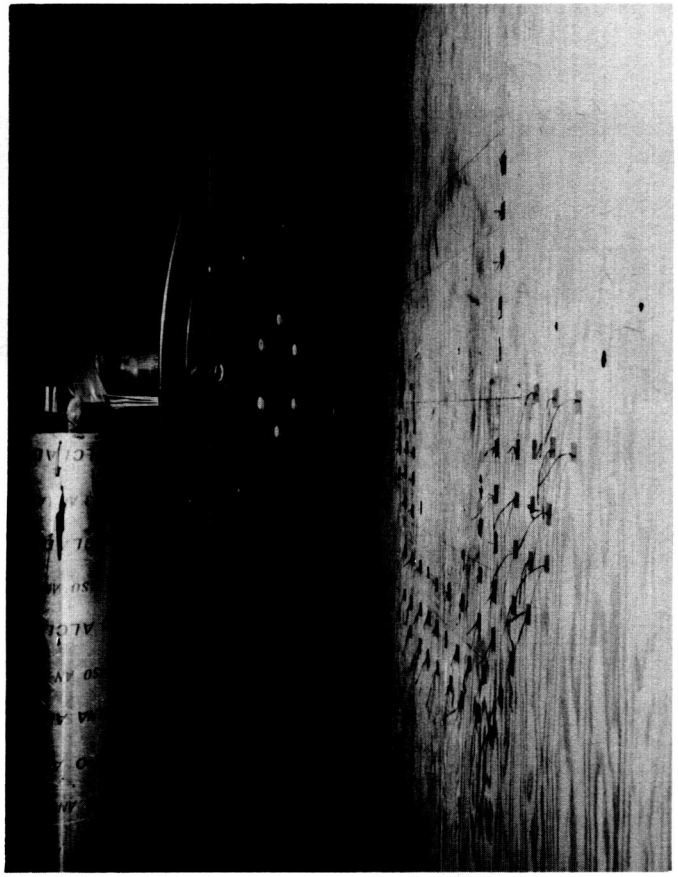

A-24890

(b) Circular wing at positive angle of attack, showing annular nozzle in lower surface.

Figure 2.- Photograph of the model installed in the Ames 7- by 10-foot wind tunnel.

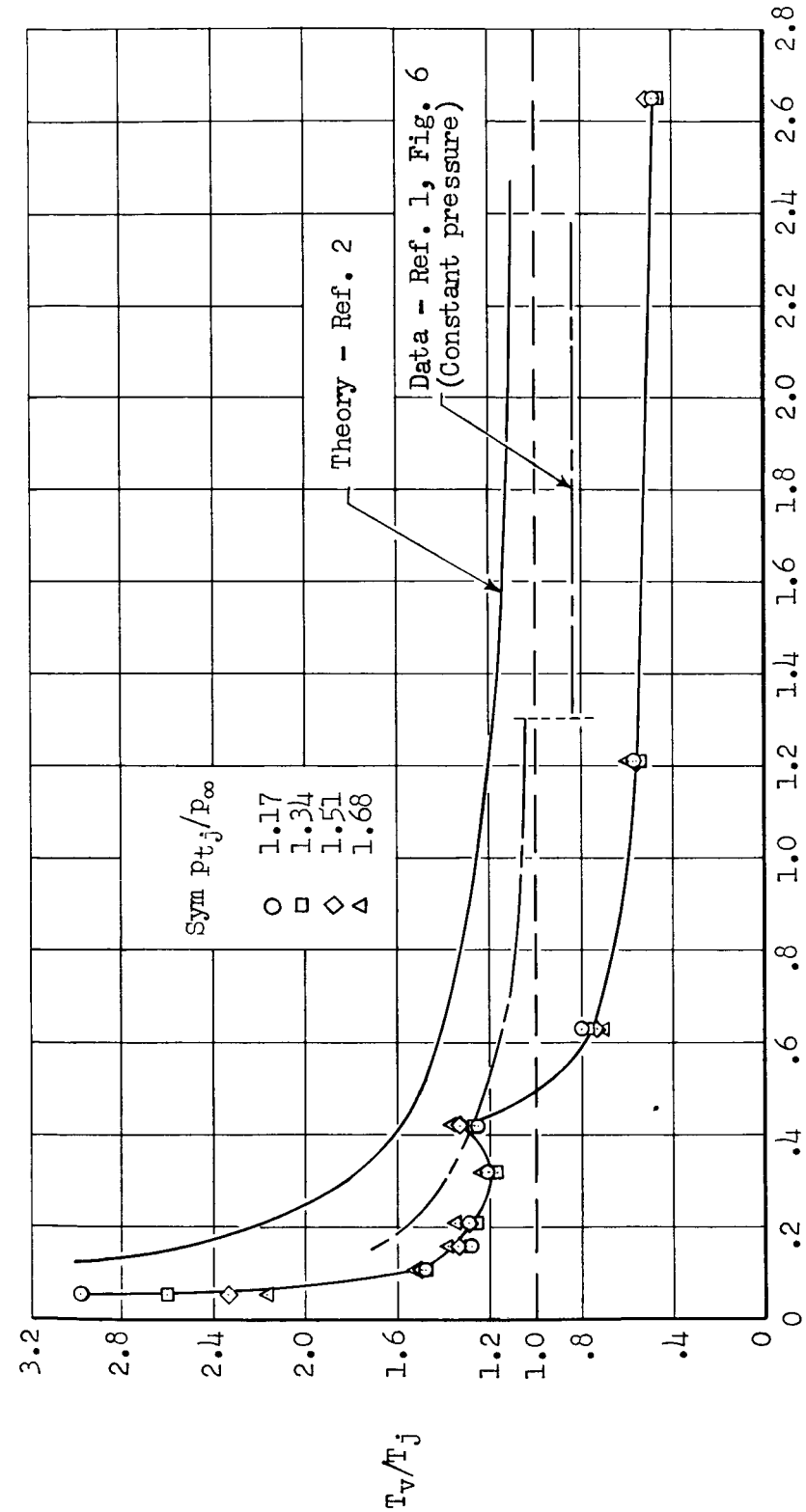

Figure 3.- Variation of vertical thrust-momentum ratio with altitude for the model operating at zero forward speed; $\alpha = 0^\circ$.

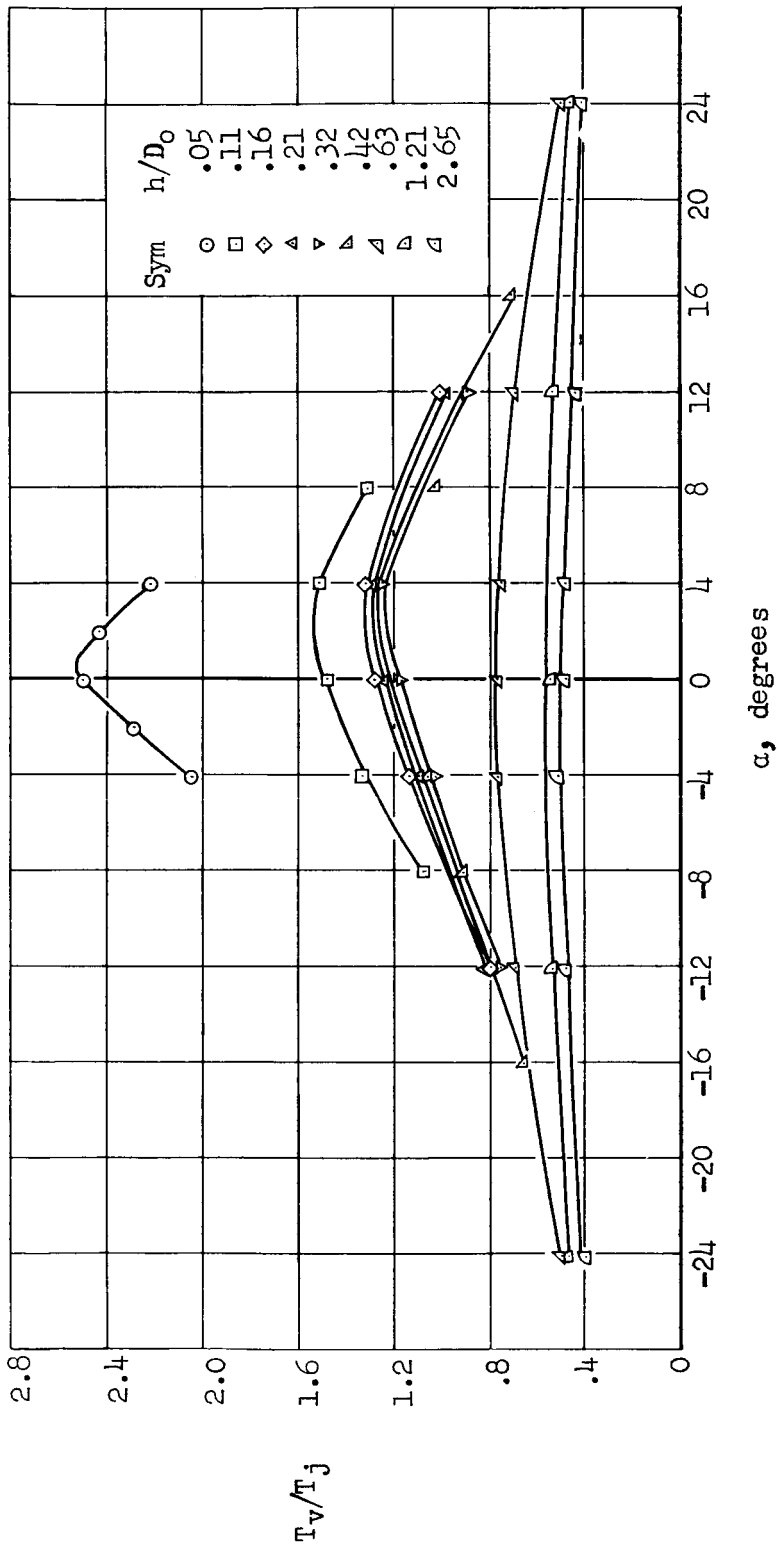

(a) Vertical thrust-momentum ratio.

Figure 4.- Effect of angle of attack on the model's performance at zero forward speed; $P_{t_j}/P_\infty = 1.34$.

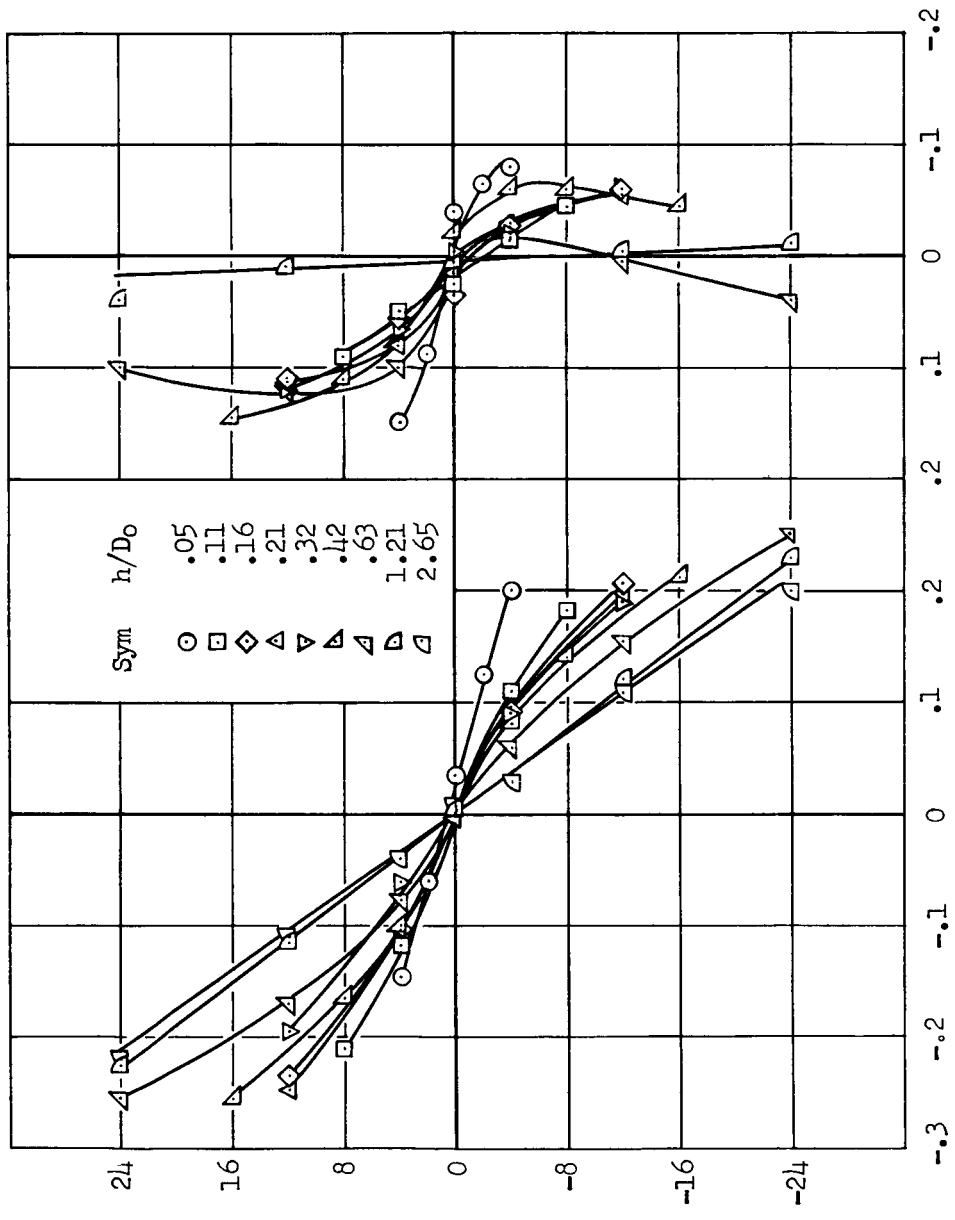

(b) Horizontal thrust-momentum ratio and pitching moment.

Figure 4.- Concluded.

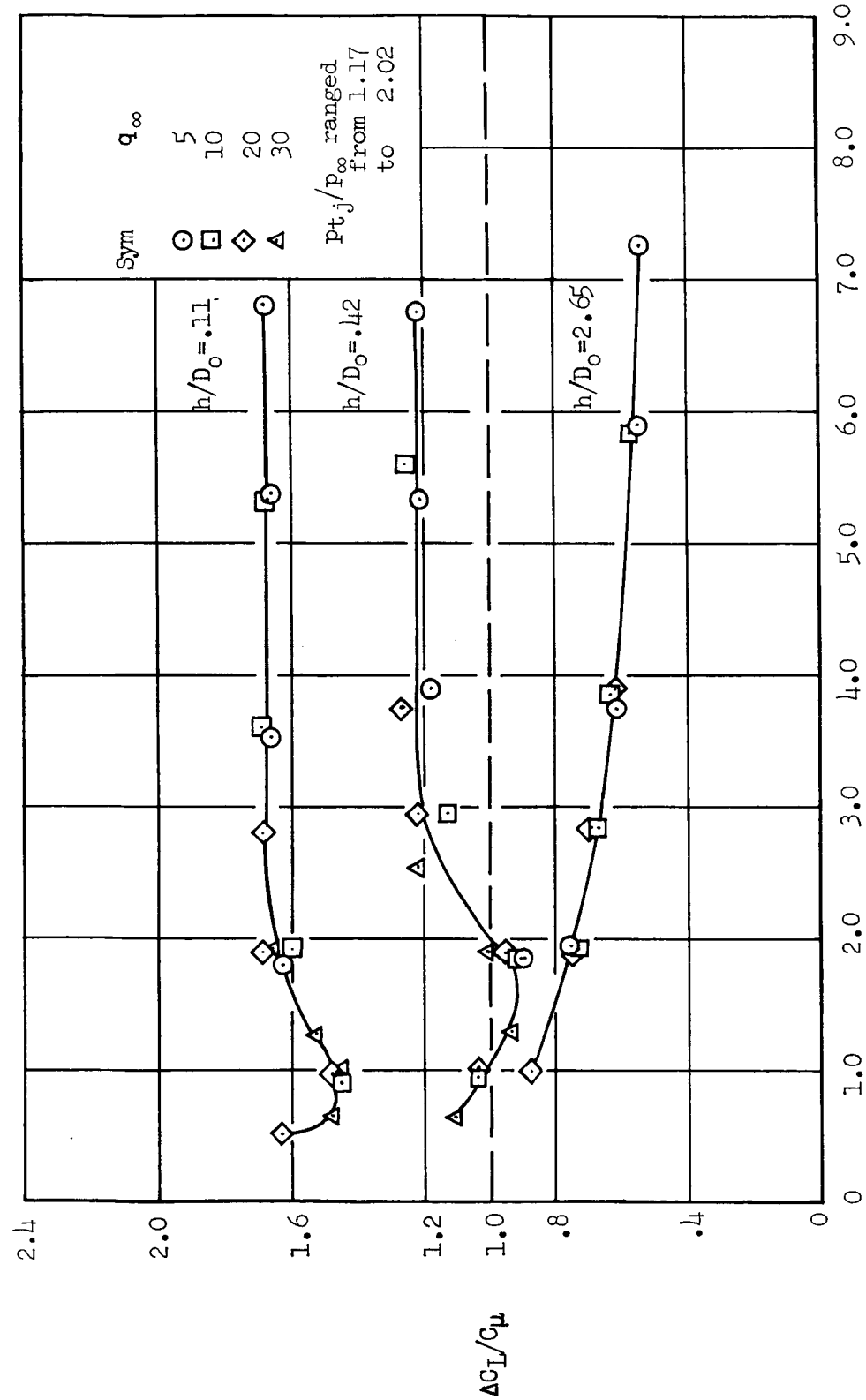

Figure 5.- Correlation of vertical thrust-momentum ratio with jet momentum coefficient; $\alpha = 0^o$.

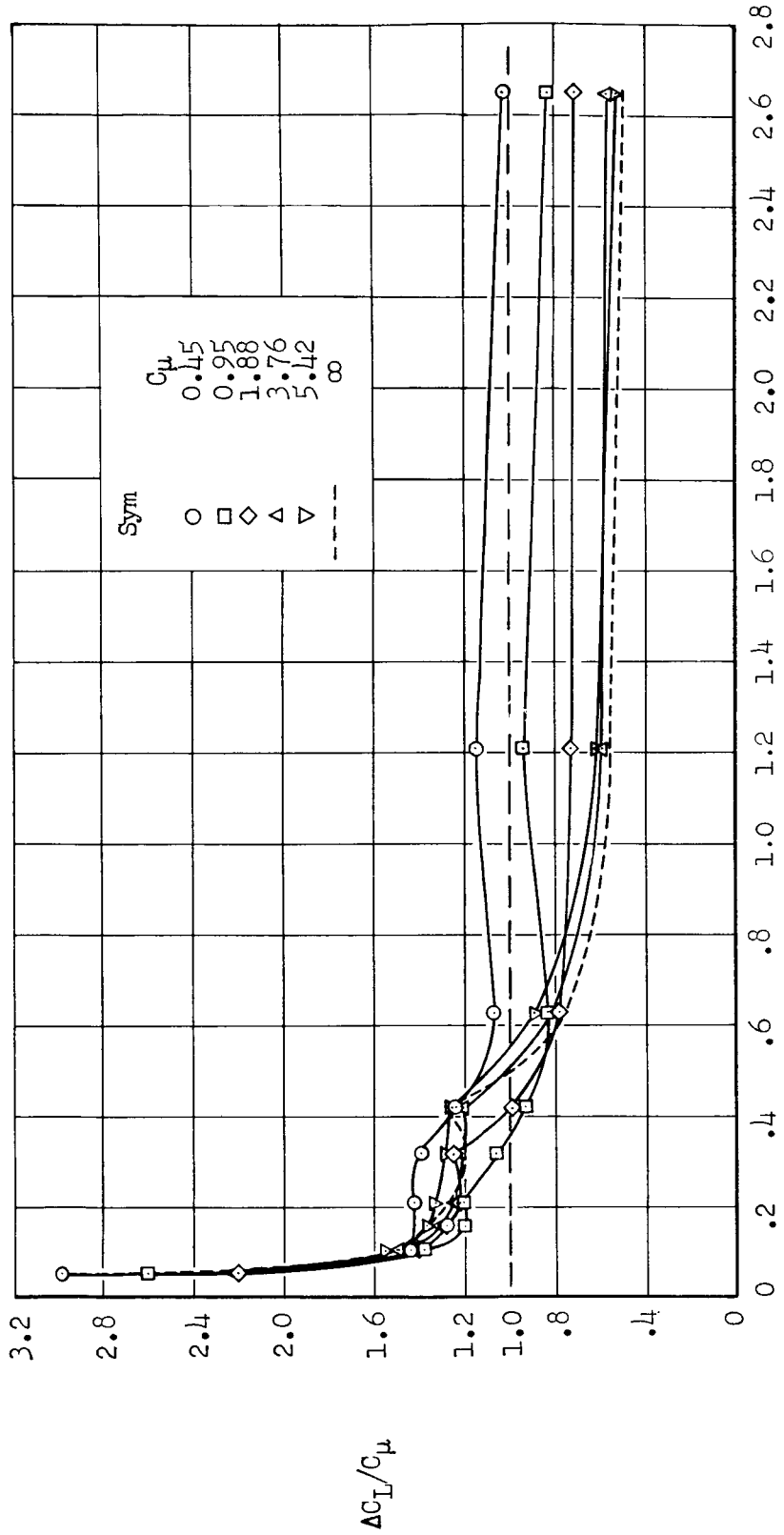

Figure 6.- Effect of C_μ on the model's vertical thrust variation with altitude; $\alpha = 0^o$.

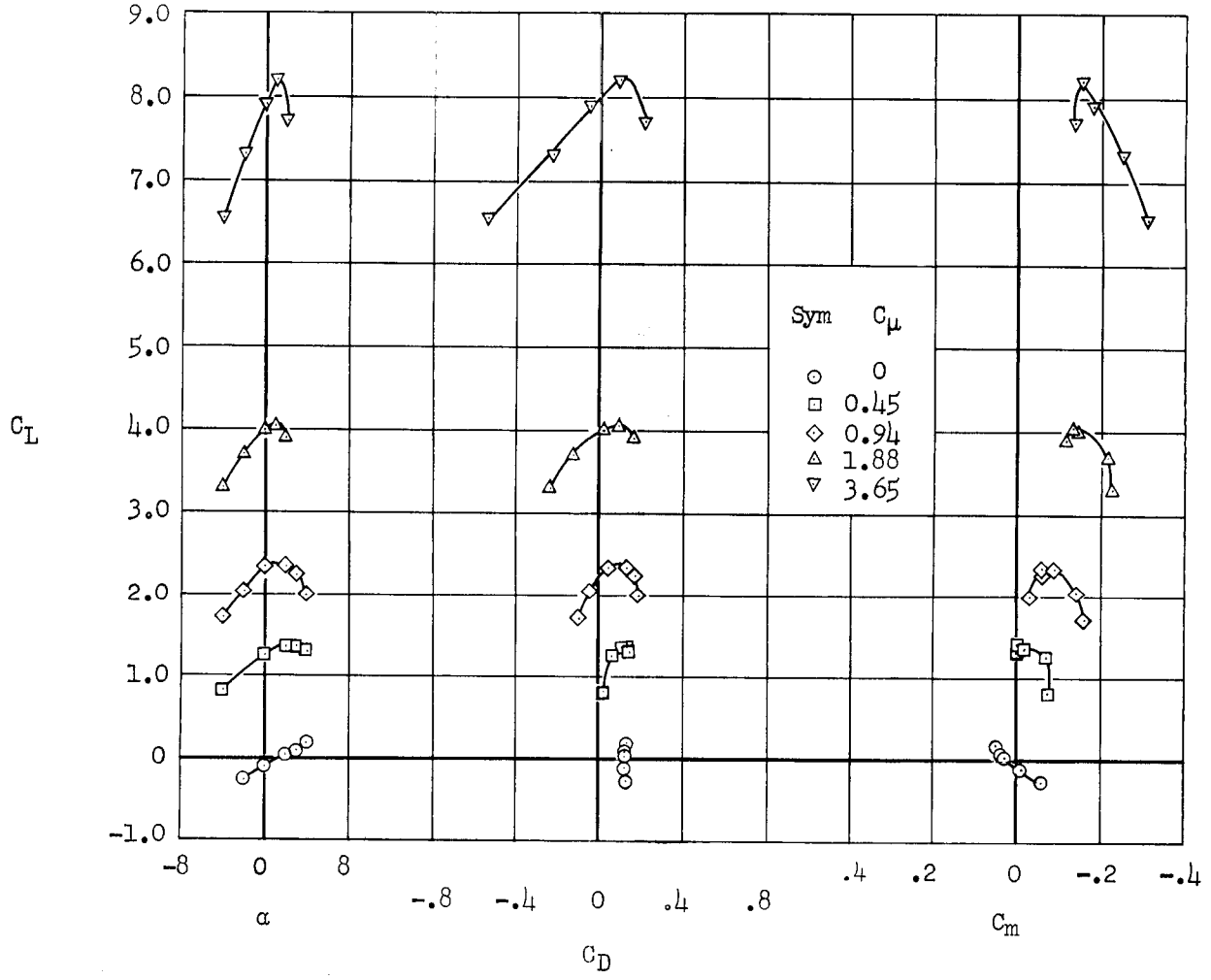

(a) $h/D_o = 0.05$.

Figure 7.- Effect of C_μ on the longitudinal characteristics of the model.

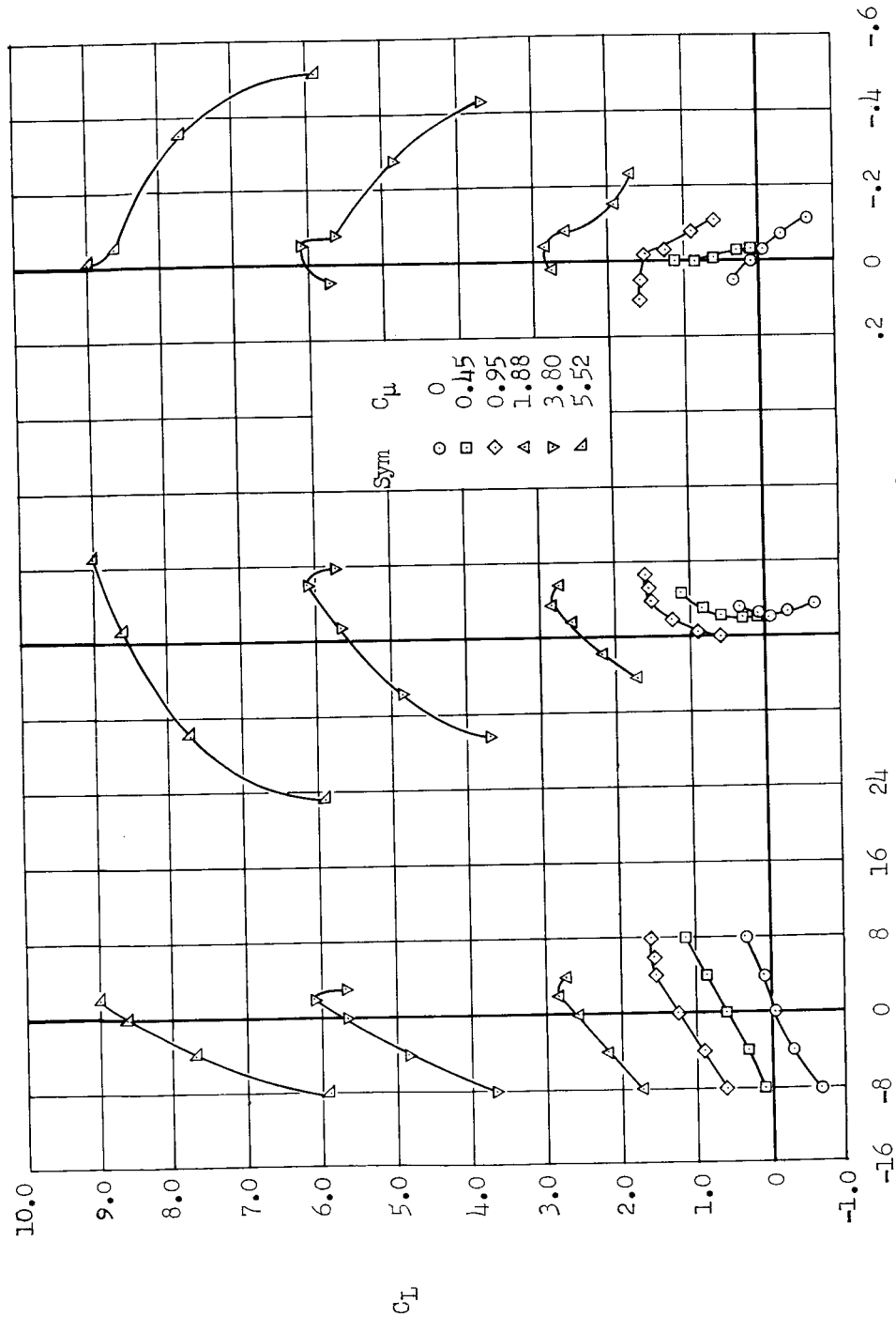

(b) $h/D_o = 0.11$

Figure 7.- Continued.

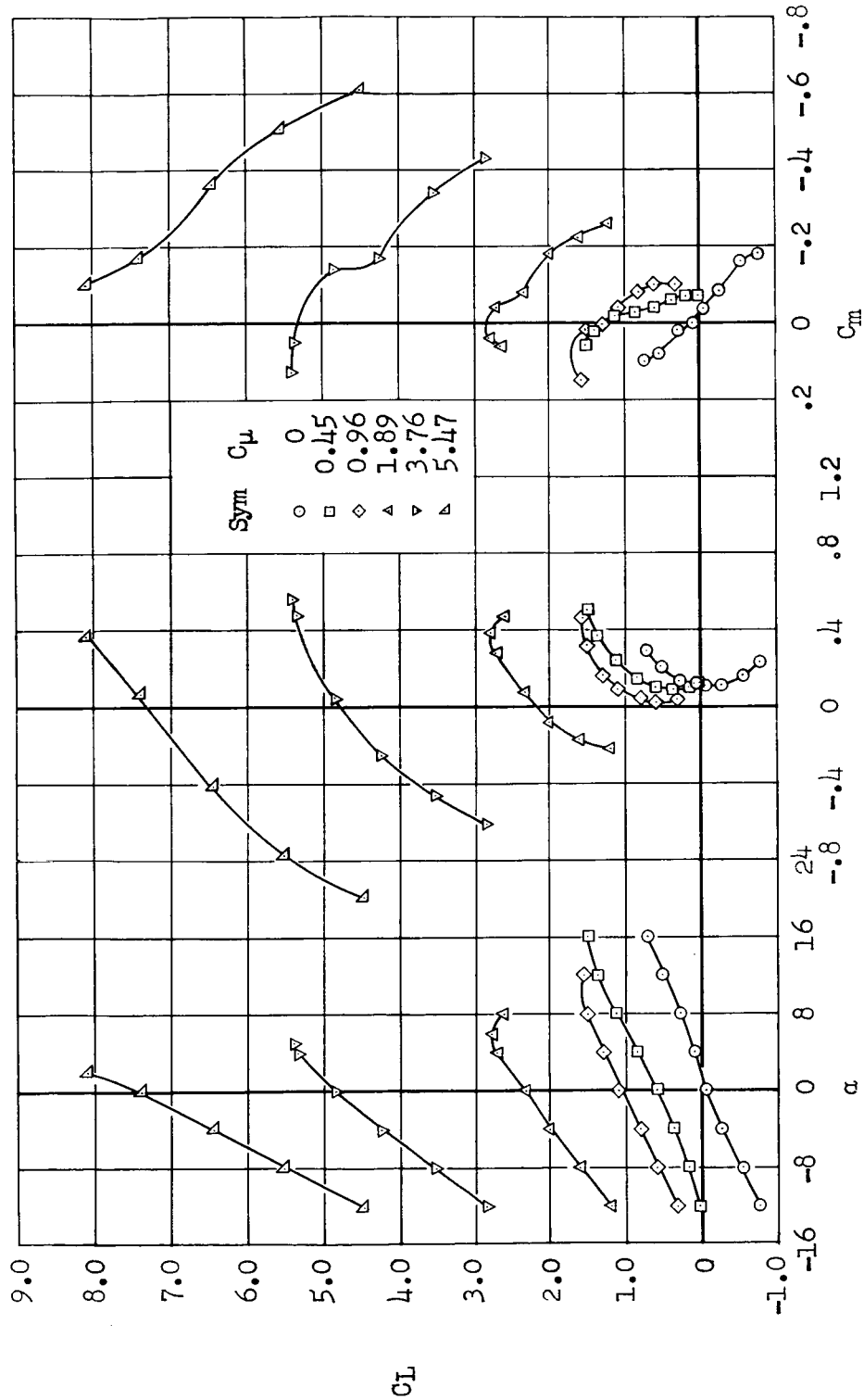

(c) $h/D_o = 0.16$

Figure 7.- Continued.

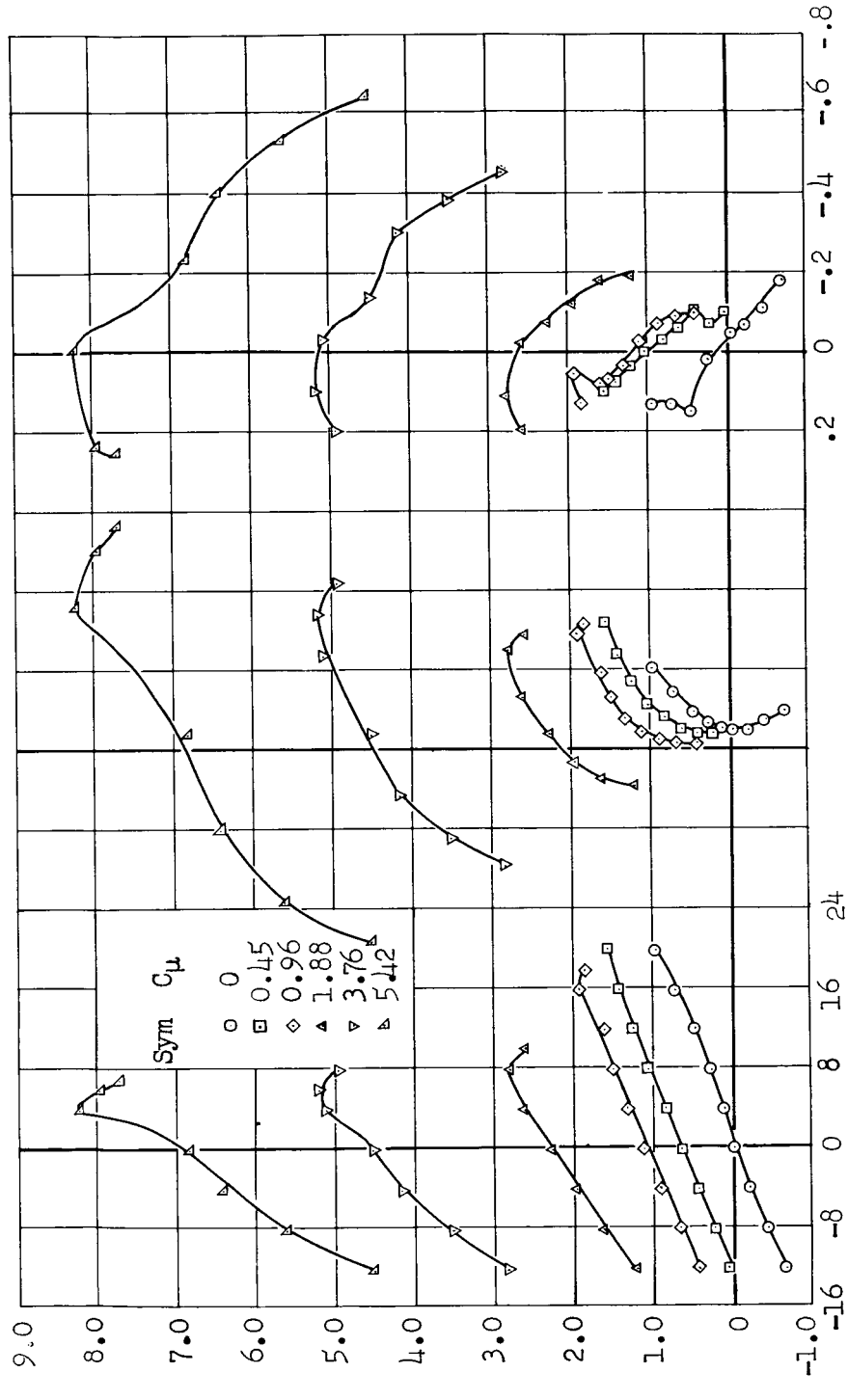

(d) $h/D_o = 0.21$

Figure 7.- Continued.

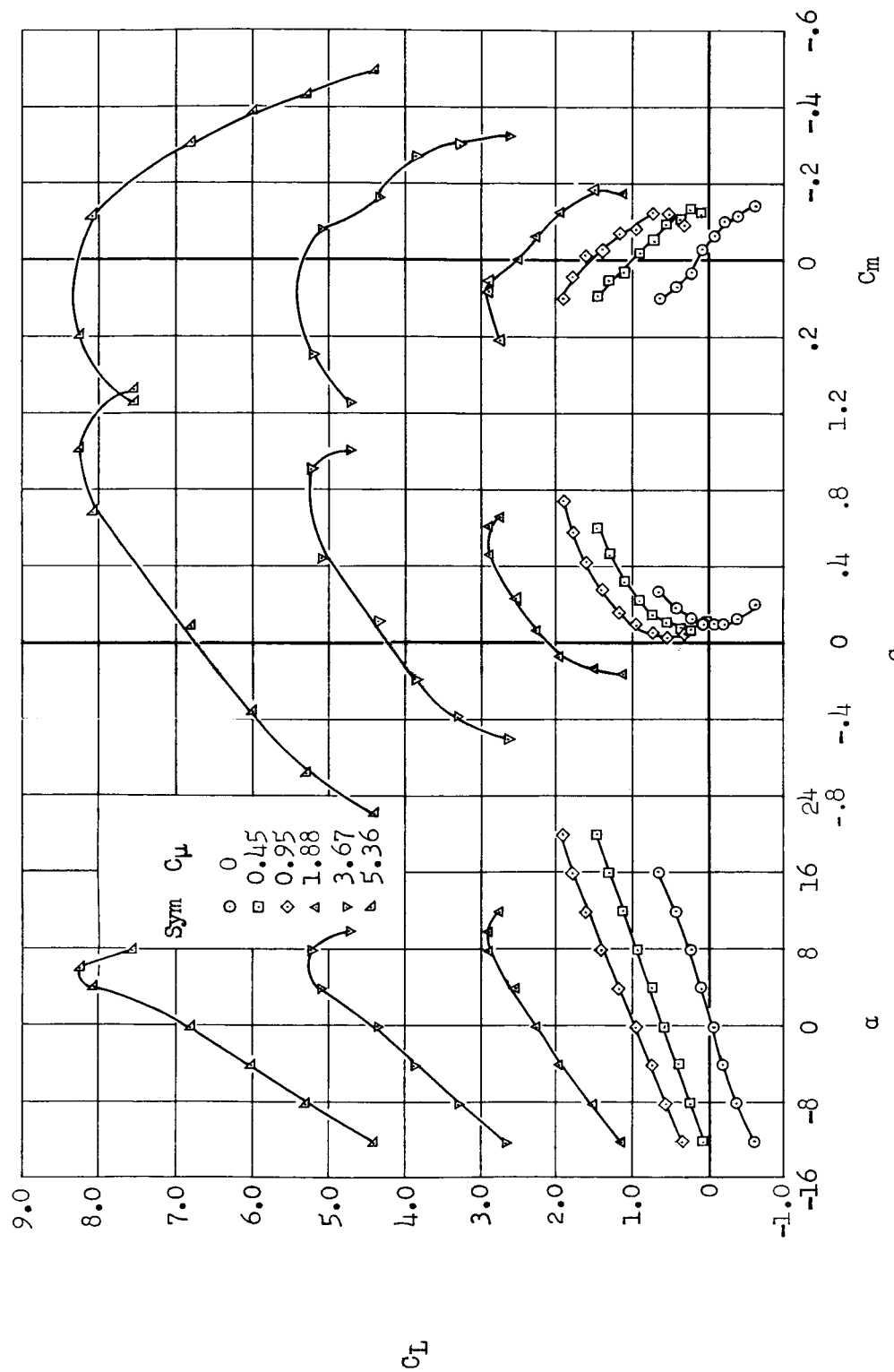

(e) $h/D_o = 0.32$

Figure 7.- Continued.

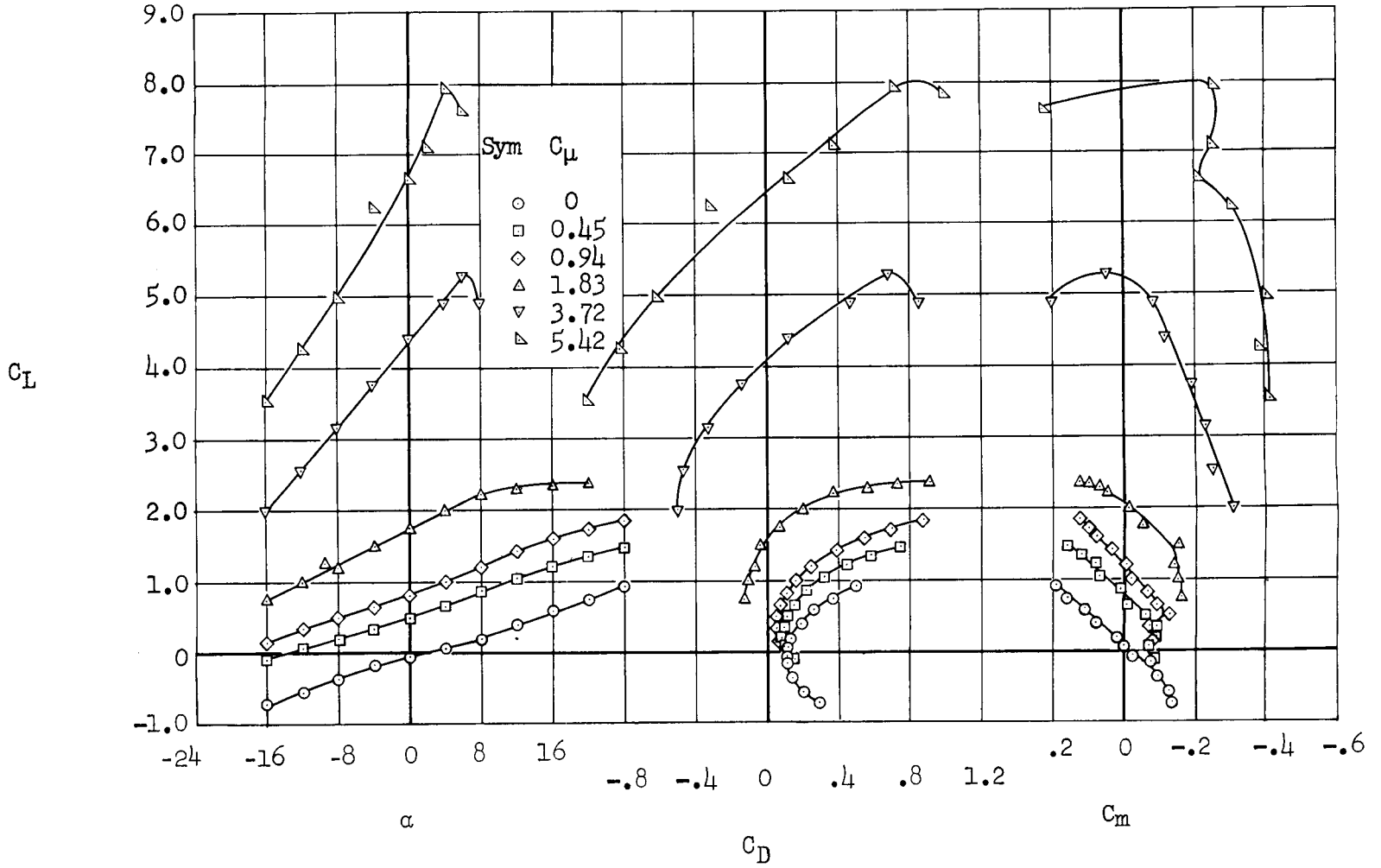

(f) $h/D_o = 0.42$

Figure 7.- Continued.

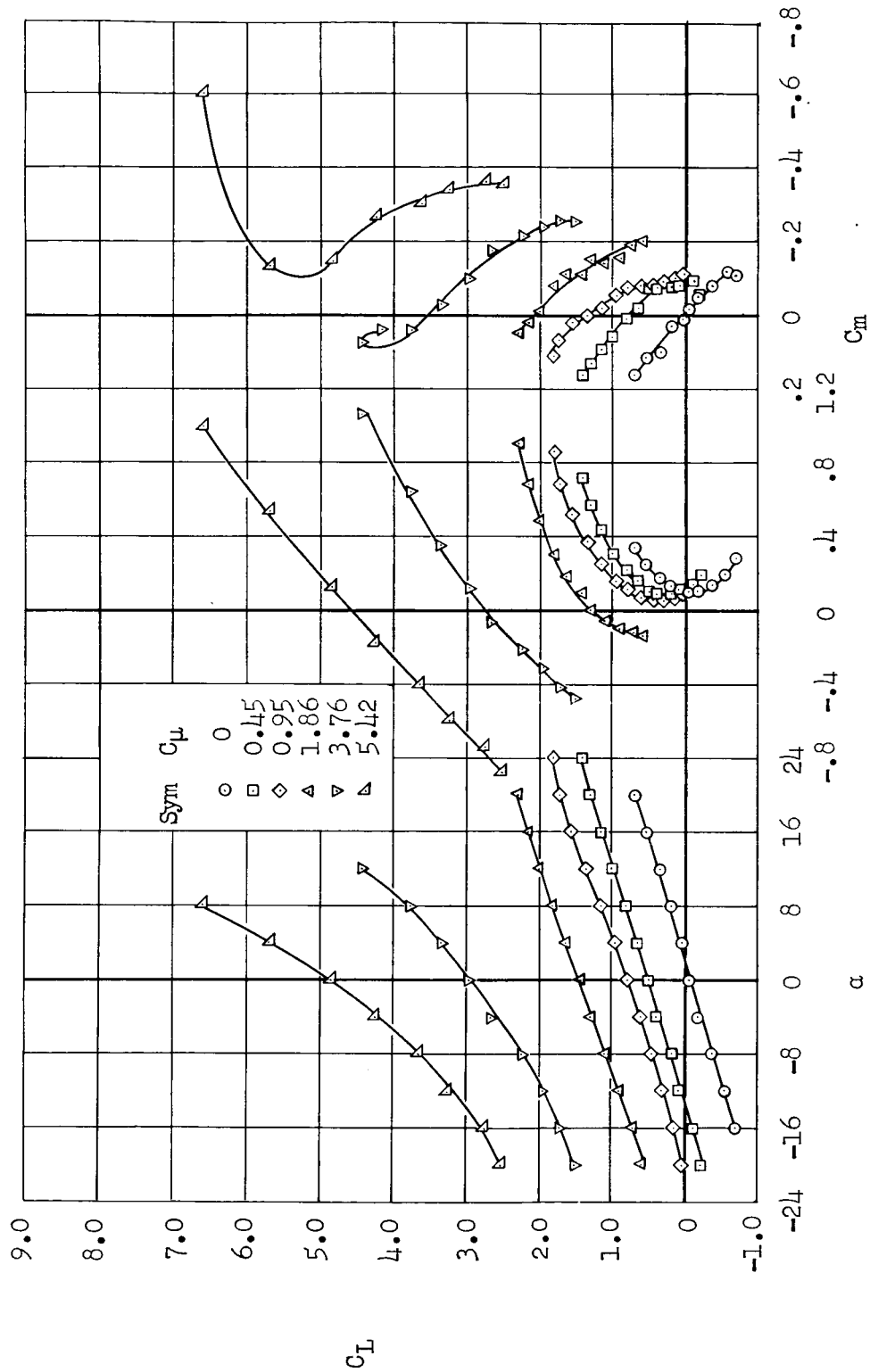

(g) $h/D_0 = 0.63$

Figure 7.- Continued.

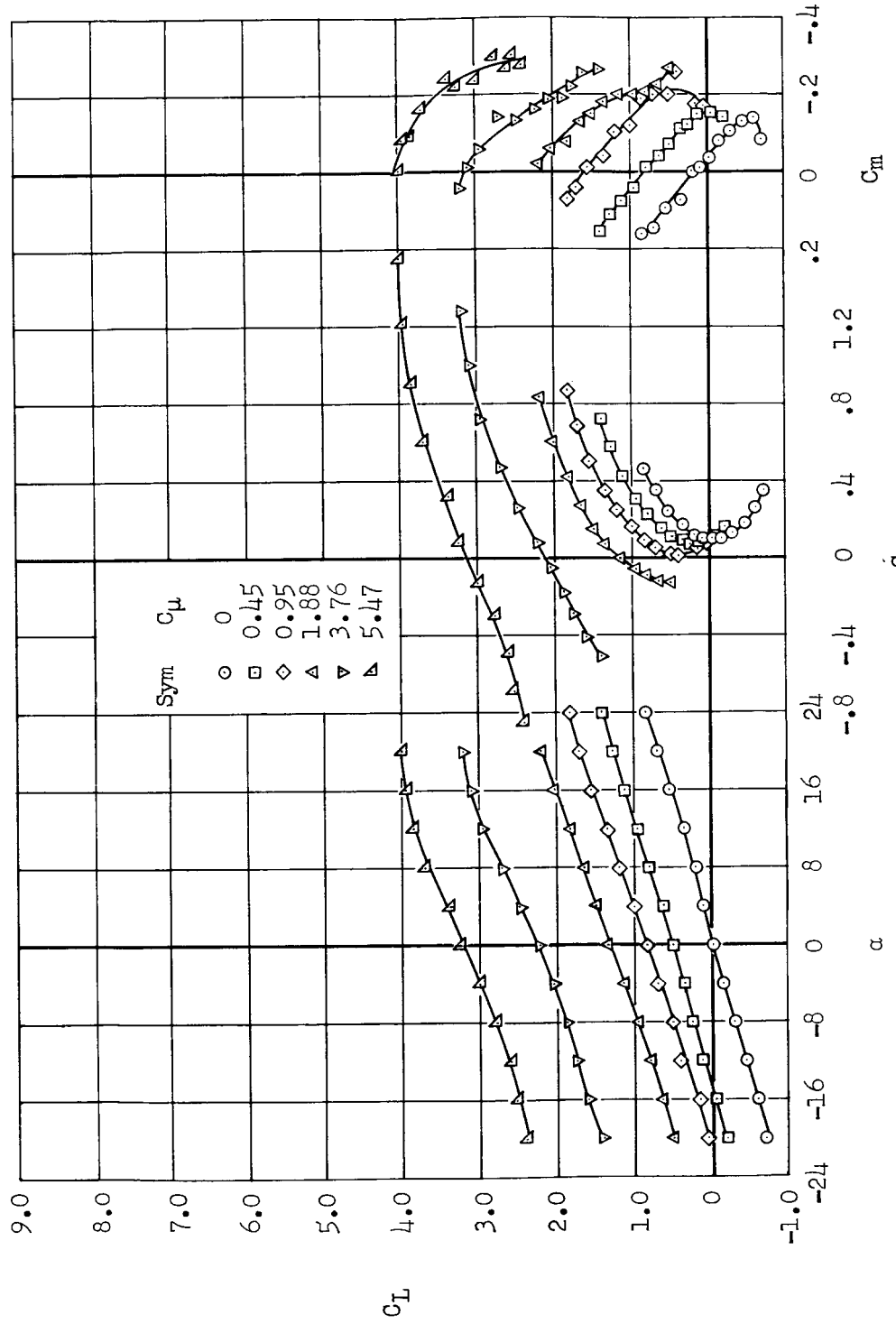

(h) $h/D_o = 1.21$

Figure 7.- Continued.

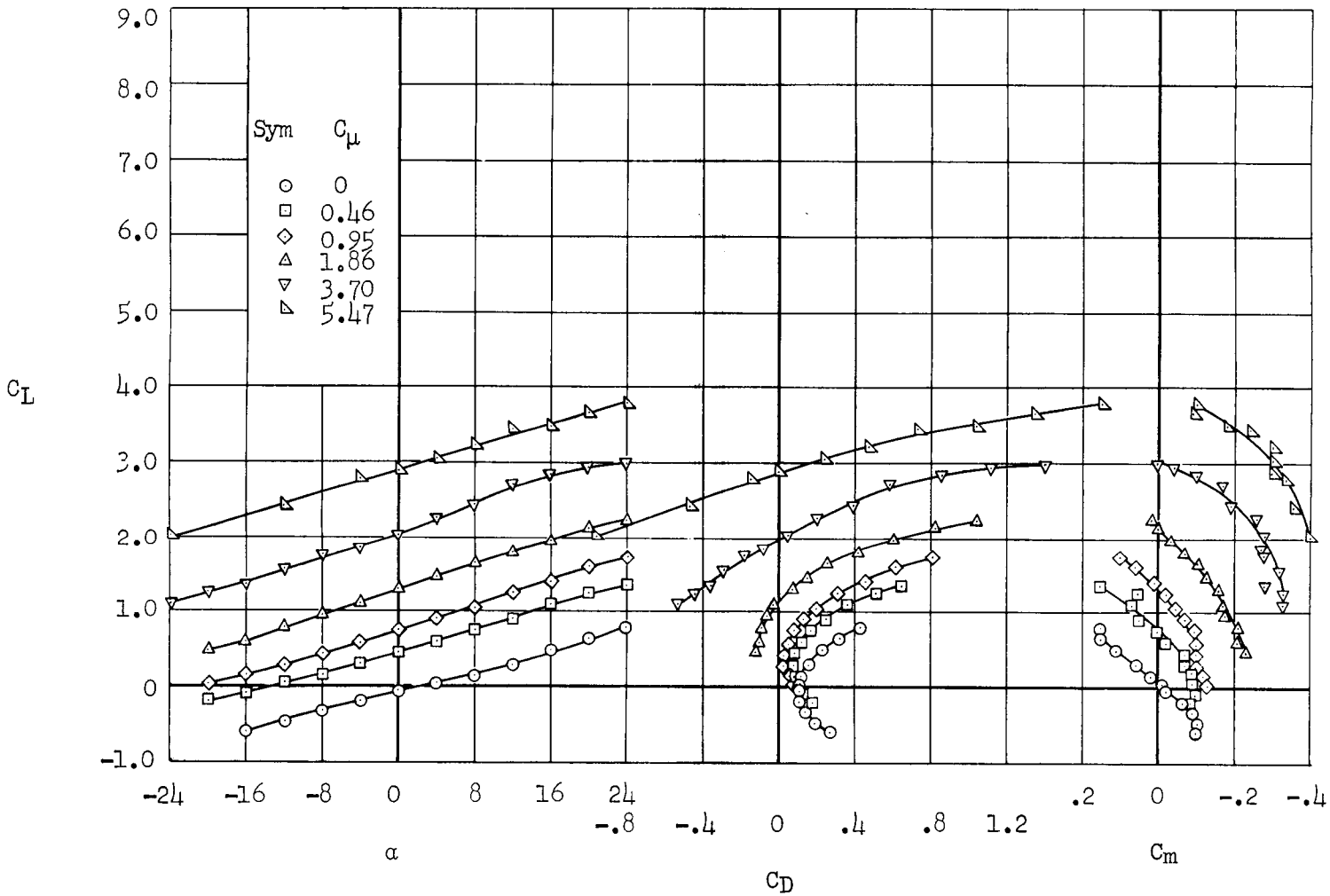

(i) $h/D_o = 2.65$

Figure 7.- Concluded.

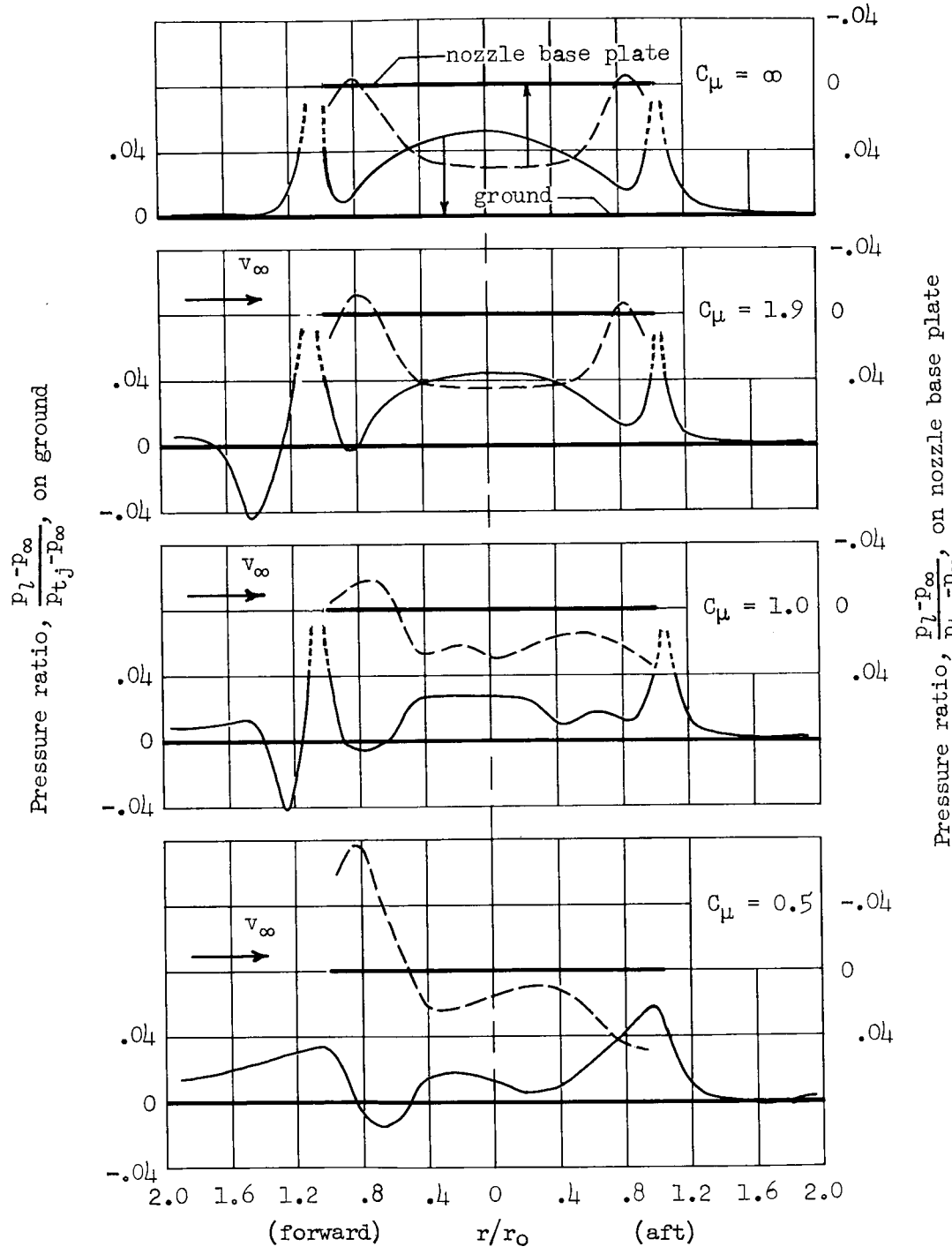

(a) Effect of C_μ with $\alpha = 0^o$.

Figure 8.- Pressure profiles on ground and nozzle base plate for $h/D_o = 0.11$.

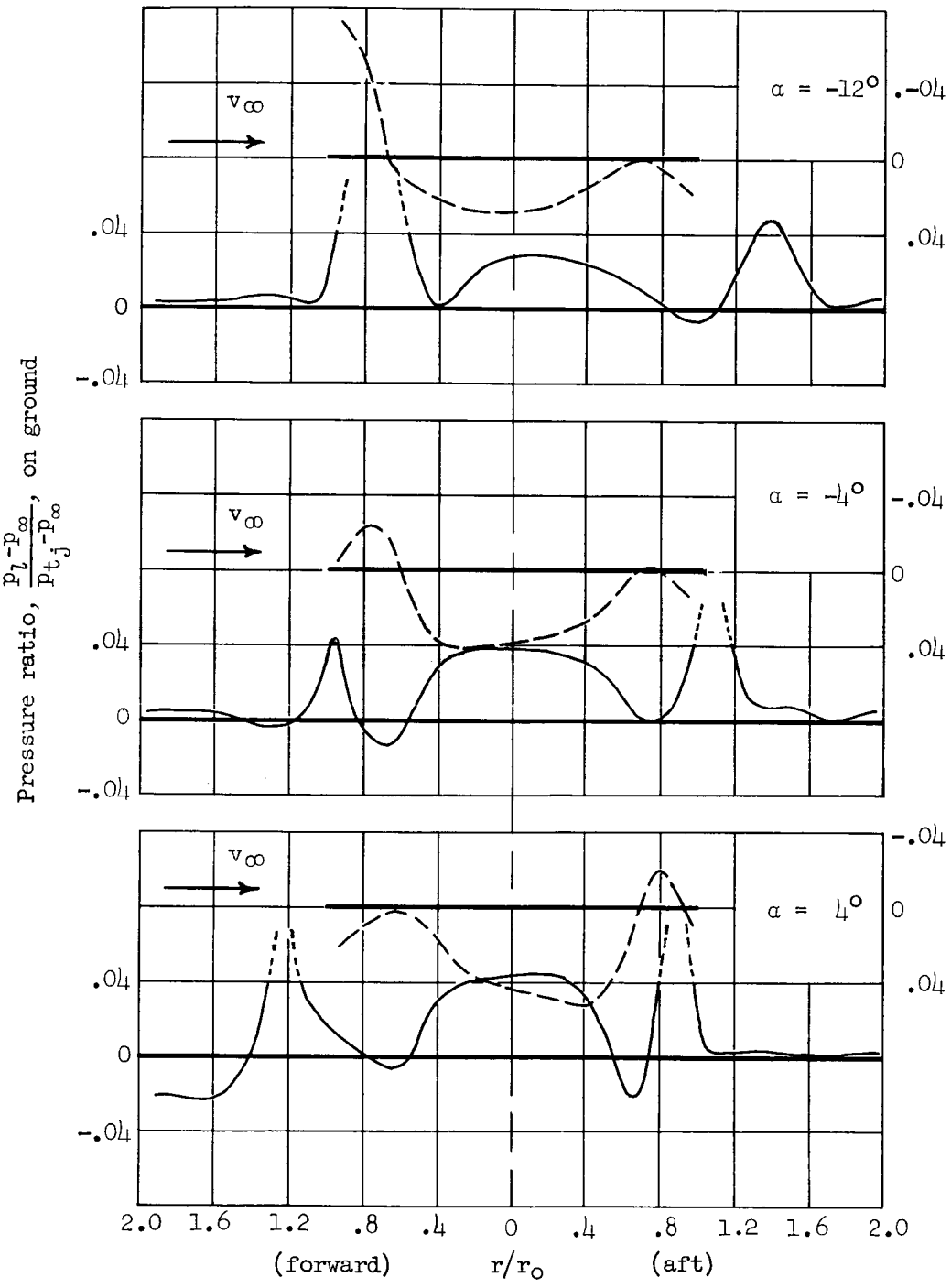

(b) Effect of α with $C_\mu = 1.9$.

Figure 8.- Continued.

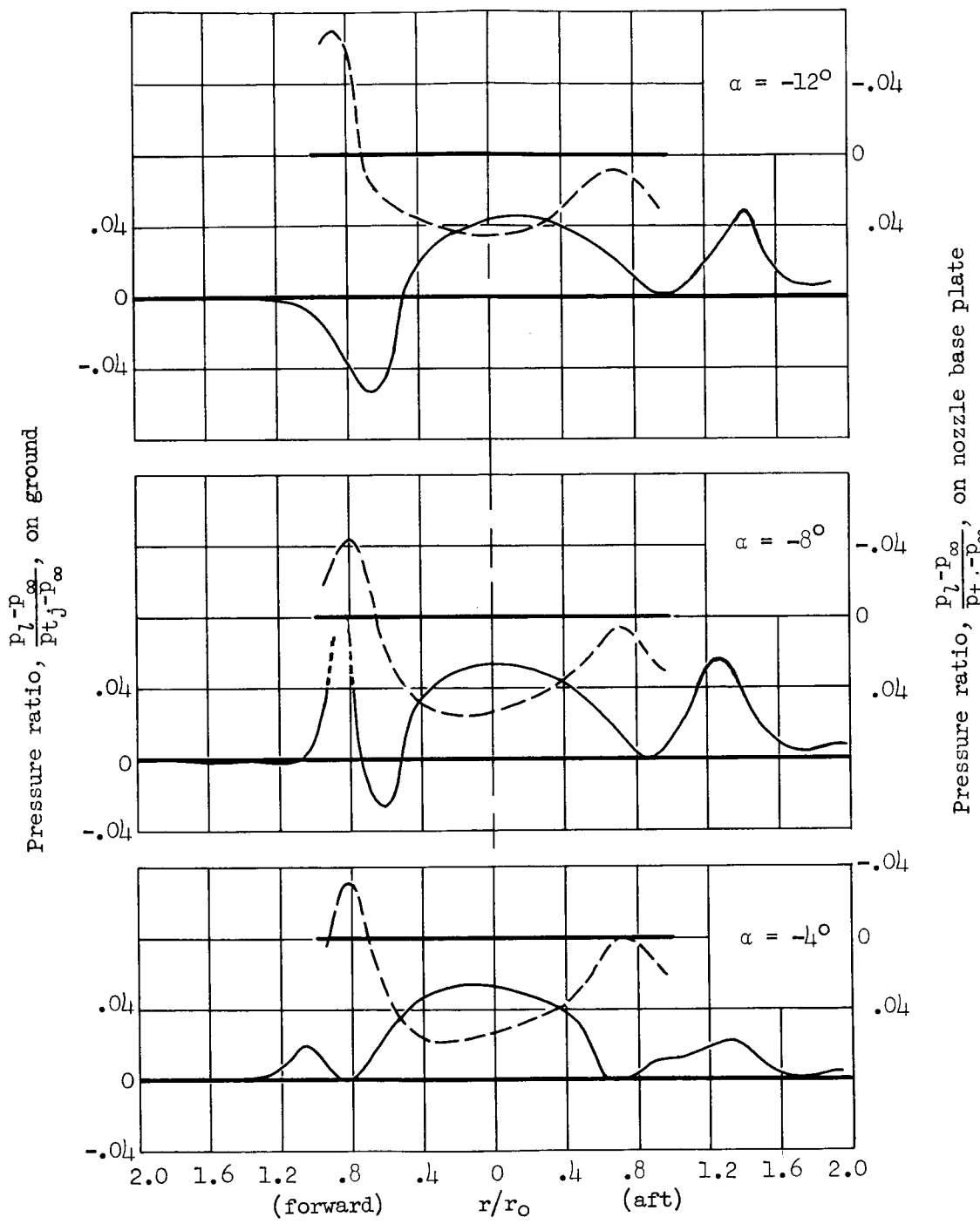

(c) Effect of α with $C_\mu = \infty$.

Figure 8.- Concluded.

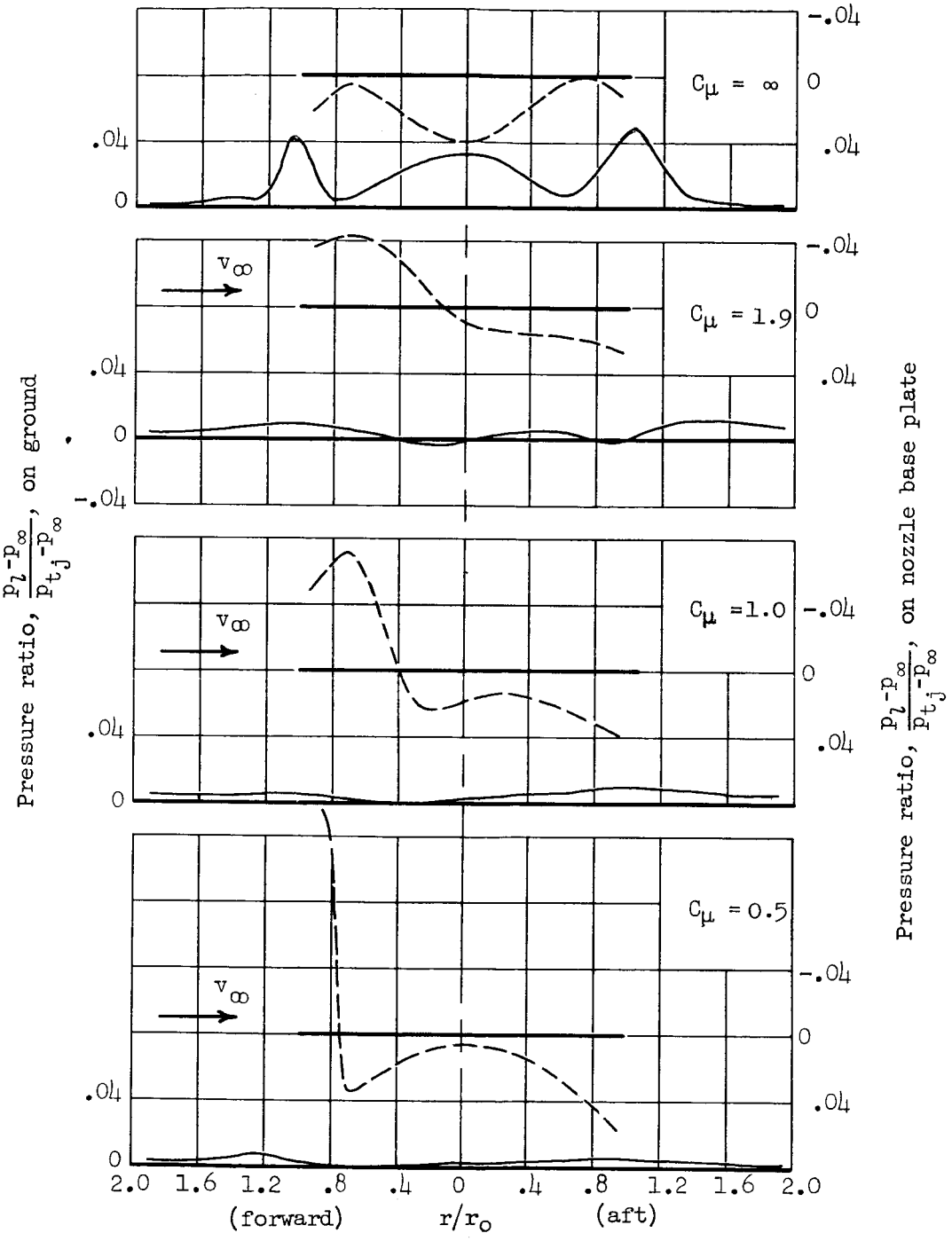

(a) Effect of C_μ with $\alpha = 0^o$.

Figure 9.- Pressure profiles on ground and nozzle base plate for $h/D_o = 0.42$.

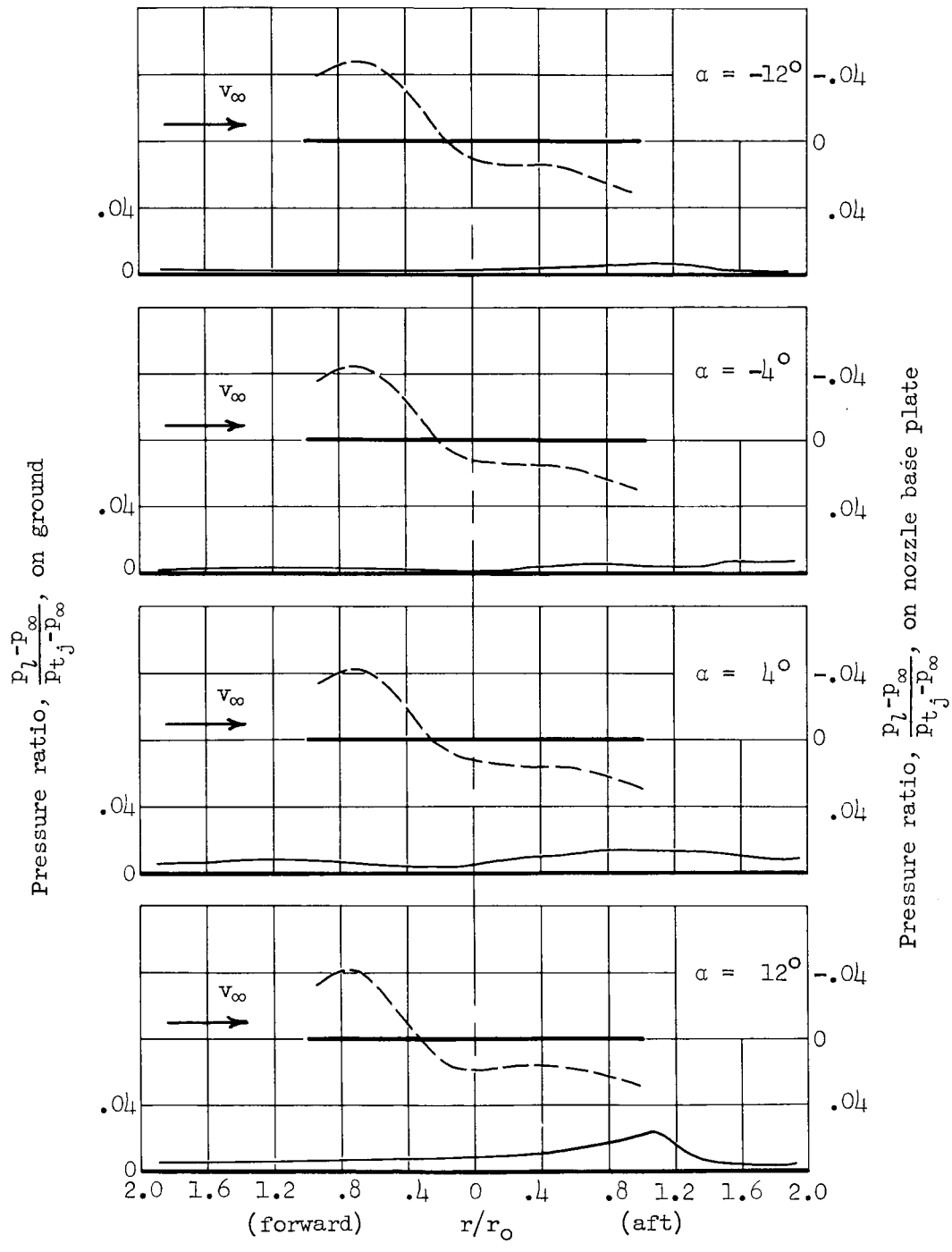

(b) Effect of α with $C_\mu = 1.9$.

Figure 9.- Continued.

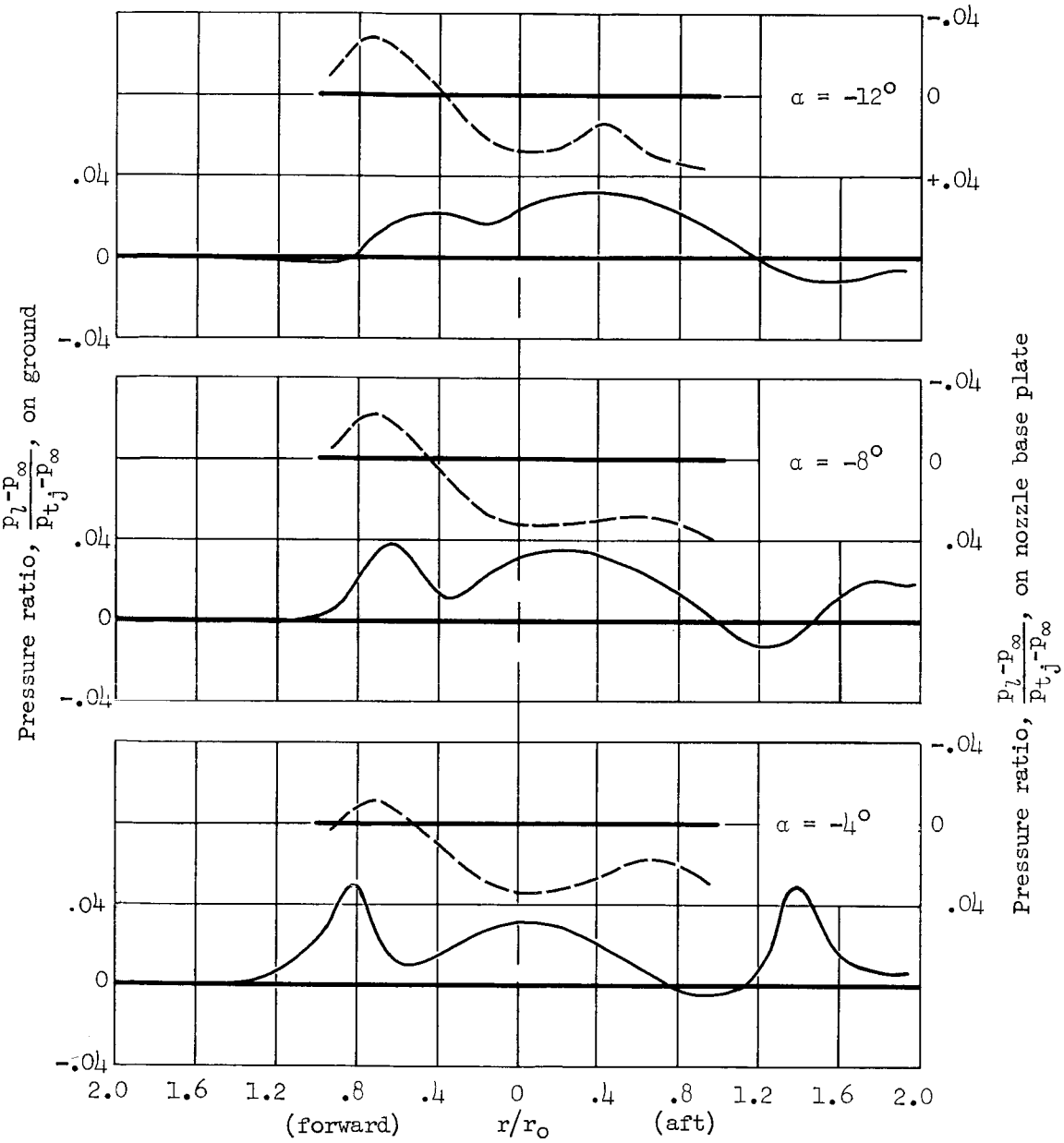

(c) Effect of α with $C_\mu = \infty$.

Figure 9.- Concluded.

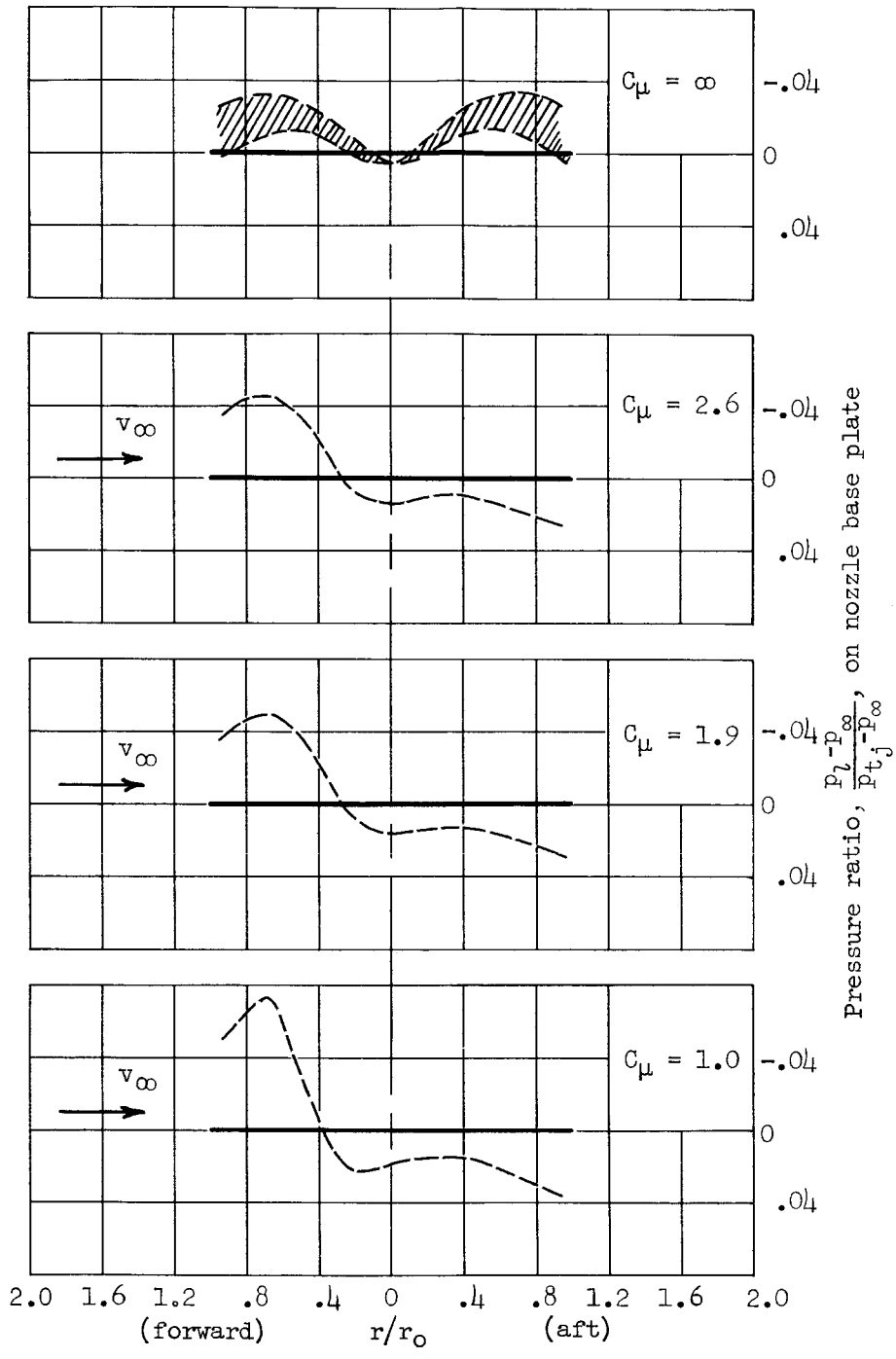

(a) Effect of C_μ with $\alpha = 0^o$.

Figure 10.- Pressure profiles on nozzle base plate for $h/D_o = 2.65$.

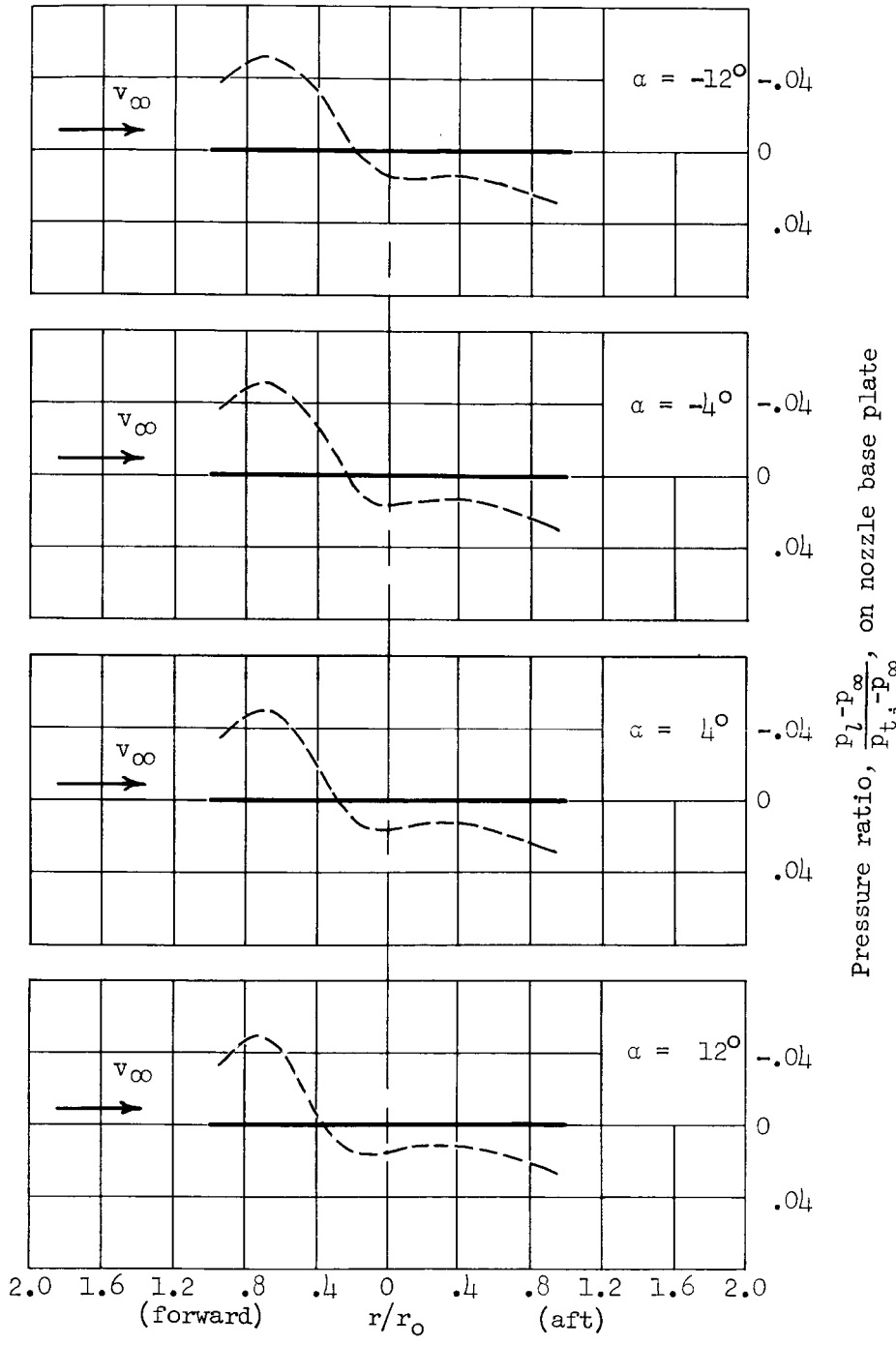

(b) Effect of α with $C_\mu = 1.9$.

Figure 10.- Concluded.